Published in final edited form as:
J Geophys Res Planets. 2016 October ; 121(10): 1865–1884. doi:10.1002/2016JE005128.

Space Weathering on Airless Bodies

Carle M. Pieters and
Department of Earth, Environmental, and Planetary Sciences, Brown University, Providence, RI 02912, Phone: 401-863-2417

Sarah K. Noble
Planetary Science Division, NASA Headquarters, Washington DC, 20546, one: 202-358-2492

Abstract

Space weathering refers to alteration that occurs in the space environment with time. Lunar samples, and to some extent meteorites, have provided a benchmark for understanding the processes and products of space weathering. Lunar soils are derived principally from local materials but have accumulated a range of optically active opaque particles (OAOpq) that include nanophase metallic iron on/in rims formed on individual grains (imparting a red slope to visible and near-infrared reflectance) and larger iron particles (which darken across all wavelengths) such as are often found within the interior of recycled grains. Space weathering of other anhydrous silicate bodies, such as Mercury and some asteroids, produce different forms and relative abundance of OAOpq particles depending on the particular environment. If the development of OAOpq particles is minimized (such as at Vesta), contamination by exogenic material and regolith mixing become the dominant space weathering processes. Volatile-rich bodies and those composed of abundant hydrous minerals (dwarf planet Ceres, many dark asteroids, outer solar system satellites) are affected by space weathering processes differently than the silicate bodies of the inner solar system. However, the space weathering products of these bodies are currently poorly understood and the physics and chemistry of space weathering processes in different environments are areas of active research.

1 Introduction

Materials exposed to the harsh space environment are gradually altered in both physical and compositional properties to some degree. The generic definition of space weathering refers to this process. Simply stated, *space weathering* is the gradual alteration of materials when they are exposed to a variety of natural processes that occur in the space environment. Understanding the causes and the effects of space weathering on different planetary surfaces, however, is not simple. There are multiple simultaneous processes that can and do alter surface materials on bodies that are not protected by an atmosphere. Related concepts found throughout the literature are soil maturity and exposure age. *Soil maturity* is a relative term, commonly used for the Moon, that is intended to evaluate the degree to which a given surface soil has accumulated space weathering products [e.g. Morris 1978; Lucey et al., 2000]. On the other hand, *exposure age* is a quantitative laboratory measure of how long a rock or soil grain has been exposed to space, and is based on precise measurements of accumulated products such as solar wind noble gases or cosmic ray tracks [e.g., Zinner 1980; Berger and Keller 2015a]. The discussion presented here focuses on space weathering

processes and their alteration products as currently observed for airless bodies of the solar system.

Space weathering processes can be loosely grouped in two broad categories related to (I) random impacts by small particles or debris found throughout the solar system or (II) irradiation by electromagnetic radiation or atomic particles from the Sun, galactic sources, or magnetosphere. The wide range of impact and irradiation sub-categories spawn numerous specific processes, many of which can be evaluated more directly with observations, experiments, and/or modeling. The energy released in impacts, for example, break apart larger particles into smaller particles (comminution), but it also melts and vaporizes some of the host and impactor material (which leads to a range of possible alteration products). Depending on impact parameters (velocity, target composition, geometry, etc.), a portion of the impactor may be retained and mixed with the host in the combined product. Repeated impacts of various sizes also stir and mix previously processed regolith particles to different depths (known as gardening a soil), so the actual time spent on the surface by an individual grain varies stochastically. At the atomic or molecular scale, individual grains residing on the surface are awash in energetic solar wind atoms or ions leading to a release and/or rearrangement of surface components by sputtering. The original crystalline structure of the uppermost surface of a grain can record and be damaged by intense solar UV radiation and energetic cosmic rays. Diurnal thermal cycling occurs from solar insolation during rotation (rapid or slow) of the planetary body. This not only can lead to structural fatigue of surface materials, but may also alter composition through loss of volatile species by radiant heating or sublimation. With time, a host of alteration products accumulate on the surface and are recycled multiple times through several of the processes mentioned above and illustrated in Figure 1.

Due to the diversity of environments and type of materials comprising planetary surfaces, space weathering can have many forms and is inherently controlled by which processes are most active in a specific situation. Combined products of space weathering processes are necessarily a function of *location* in the solar system (impact speed and flux, radiation environment, and temperature), *type of planetary surface* (composition, size, and texture of the host), and *length of time* a surface is exposed. Experience from the Moon and virtually all planetary bodies visited to date indicates that ancient surfaces consist of coarse to fine particulate material. Boulders and outcrops of rocky or coherent solid material are common, but a particulate regolith develops with time. From our current experience, it is largely the regolith that accumulates and records the principal effects of space weathering.

As highlighted below, currently the regolith of two extraterrestrial bodies has been directly sampled (the Moon and the near-Earth asteroid Itokawa), and both of these bodies have evolved near 1 AU. These samples and the ongoing detailed analyses in Earth-based laboratories provide a cornerstone for recognizing and understanding key aspects of several space weathering effects. Using the insights gained from these samples, it is often possible to extrapolate understanding of weathering processes to bodies for which we have only remote data. A handful of additional bodies have been visited by spacecraft and studied in detail for extended periods with orbiting remote sensors (Mercury, Eros, Vesta, and recently dwarf planet Ceres and comet Churyumov-Gerasimenko). The satellites of Mars, Jupiter,

and Saturn, have been studied to lesser degrees through the decades by multiple flybys of instrumented spacecraft. Seven additional asteroids have been observed with instruments during a single flyby of a spacecraft (usually on its way elsewhere for its prime mission). Most recently, the most distant solar system objects visited, Pluto and its satellites, have revealed some of their secrets. The amount and type of data now available to study the surfaces of airless bodies is exceptional - but it is also extremely uneven in character and quality. Summarized in the following sections are the various forms of space weathering that are now recognized (or hypothesized) based on the clues currently available from the data in hand.

A few scientific debates have arisen about processes and products of space weathering, largely due to the inherent complexity of the natural environment. One of the earliest issues centered on interpretation of observed properties of a large class of asteroids, the so called ‘S-type’ asteroids [Bell *et al.,* 1989; Chapman 1996; 2004]. On the one hand, principal minerals identified on the surfaces of these asteroids from near-infrared telescopic reflectance spectra were found to be low-Ca pyroxene and olivine, suggesting that these asteroids are comparable to the most common type of meteorite that falls to Earth, the ordinary chondrites. However, in detail the optical properties of the S-type asteroids and the ordinary chondrites differ in an important manner: the asteroids exhibit an overall red-sloped continuum that varies among asteroids, whereas the chondrites do not. One interpretation suggested this difference was simply due to space weathering on the asteroid's surface. An alternate interpretation was that the S-type asteroids experienced an inherently different evolution than the relatively primitive ordinary chondrites, and the distinctive optical properties of the asteroids arise from a pervasive presence of exposed iron metal that resulted from a major melting and differentiation event early in the asteroid's evolution. As discussed in the sections below, the debate over this “S-type Conundrum” was largely resolved (in favor of the space weathering interpretation). This closure became possible when 1) surface processes that produce a red-sloped continuum became understood from lunar sample analyses and experiments and 2) S-type asteroids (Gaspra, Ida, Eros, Itakowa) were visited by spacecraft, with samples returned to Earth for analyses from one (Itakowa) by the Hayabusa spacecraft.

The concept that space weathering produces a measurable effect on the surface properties of many/most airless bodies became well established with analyses of lunar samples, but understanding the physics and products of interwoven processes that are involved encompasses multiple areas of active research. For example, even at 1 AU where the Moon and near-Earth asteroids reside, discussion and experimental approaches focus on the relative effects of products from micrometeorite impacts versus those arising from solar wind interactions. Imbedded within this debate is the time scale for either process to accumulate measurable products within a continually mixed regolith. The unique advantage of being able to analyze actual lunar and asteroid regolith samples using ever increasingly sophisticated instruments in Earth-based laboratories cannot be overstated. Likewise, understanding the effects of weathering processes naturally becomes even more difficult and complex for other environments of the solar system that are less well-known.

2 Lunar Space Weathering

The history of our understanding of weathering effects on the Moon is well described in a review paper by Hapke [2001], starting with the classic Gold [1955] observation that lunar crater rays disappear over time. But it was the return of lunar soils more than 45 years ago that changed forever our understanding of the characteristics of the regolith on airless bodies and forced us to reexamine how we use optical tools to evaluate composition remotely. When Apollo soils were evaluated in Earth-based laboratories, it was quickly found that their optical properties differ greatly from those of pulverized rocks from the same site [Adams and McCord, 1970]. Natural lunar soils are darker (especially at visible wavelengths) and absorptions that are diagnostic of minerals present are considerably weaker. As illustrated in Figure 2, these same properties are found in remote measurements that compare background soil with materials freshly exposed at a young crater. The observations were irrefutable: fresh lunar materials exposed on the surface are systematically altered with time. Identifying the cause of the alteration was more difficult. Most of the early literature focused on measuring the presence of dark amorphous “glass” or “agglutinates” (the complex, dark glass-welded aggregates found in lunar soils). Unfortunately, these initial inquiries simply identified lunar products of exposure to the space environment, but did not (and could not at that time) address the complexity of these unusual materials and the physical/chemical *origin* for the observed optical effects of agglutinates and natural lunar soils. That came much later as the pieces gradually came together and data accumulated from multiple directions [e.g. Pieters *et al.*, 2000, Hapke 2001; Noble et al., 2007; Domingue *et al.*, 2014].

Cassidy and Hapke [1975] were the first to suggest that the actual culprit responsible for these optical changes on the Moon could be tiny particles of metallic iron, alternately referred to in the literature as “nanophase iron” ($npFe^0$) or “sub-microscopic iron” (SMFe). The groundbreaking transmission election microscope (TEM) studies of Keller and McKay [1993; 1997] finally resolved these particles and revealed their distribution in lunar soils. There are two distinct populations of these opaque iron grains in lunar soils: they are found distributed throughout agglutinates, and in depositional (“inclusion-rich”) rims on individual grains such as illustrated in Figure 3a. In addition to the abundant deposited rims, Keller and McKay also identified solar-wind damaged “amorphous rims”, which contain little or no $npFe^0$ and are compositionally linked to the host grain as illustrated in Figure 3b. In some cases there are “multiple” rims in which an amorphous rim is overlain by a depositional rim.

The $npFe^0$ found in the depositional rims is very small, with a range of ~1-10 nm in diameter and an average of ~3 nm [Keller and Clemett, 2001], while the iron particles in agglutinates comes in a much wider range of sizes, up to hundreds of nanometers in diameter. Size is important because the optical changes that are attributed to space weathering are highly dependent on the size and quantity of nanophase opaques. Britt and Pieters [1994] found that finely-dispersed larger (micron-scale) particles of nickel-iron and FeS cause a reduction in reflectance throughout the visible/infrared with no apparent effect on continuum slope. It was suggested by Keller *et al*, [1998] that very small $npFe^0$ particles (<5 nm) cause spectral reddening, whereas larger particles introduce darkening without reddening. Noble *et al.* [2007] explored the effects of size and concentration of nanophase

iron by systematically impregnating a series of silica gels with different pore sizes with $npFe^0$ (Figure 4). Results quantified the earlier observations and demonstrated that small iron particles (<40 nm) cause systematic reddening and darkening across the visible/near-infrared (Vis/NIR), and larger iron particles (>40 nm) cause darkening, but not reddening, throughout the wavelength range. Lucey and Noble [2008] expanded on the Noble *et al* [2007] study by using methods developed by Hapke [1981, 1993, 2001] based on Rayleigh scattering to compute model spectra for comparison to the Noble et al. experiments. The results successfully modeled the experiments that contained small $npFe^0$ of sizes up to about 40-50 nm, however, there were significant deviations between model and experiment for samples with abundant larger particles (> 40-50 nm). The failure of the model spectra to match these spectra for larger iron particles occurs because these particles do not behave as highly efficient Rayleigh absorbers (as assumed in Hapke's [2001] model), and so cannot be modeled simply by Rayleigh scattering. A more successful modeling result is found when a Mie scattering component is added to account for the larger particles [Lucey and Riner, 2011]. This size cutoff is close to the limit of detectability of ferromagnetic resonance (FMR) for iron particles (~35 nm [Morris, 1976]), thus the standard measure of lunar soil maturity, I_s/FeO, is a measure of just the $npFe^0$ contribution and does not help quantify the larger particles (though for the Moon the two components are generally well correlated).

A detailed coordinated study of a representative suite of lunar soils from all Apollo sites was undertaken to document the petrographic, chemical, and optical properties as well as I_s/FeO values for lunar soils across a range of soil maturity. Referred to as the Lunar Soil Characterization Consortium (LSCC), this effort produced integrated detailed data for properties relevant to space weathering [Taylor *et al.* 2001; 2010]. The data document that for any given soil, values of I_s/FeO increase with decreasing particle size, and that $npFe^0$ thus principally resides on the surface of particles.

The combination of sample observations [Keller and McKay, 1993; 1997; Taylor *et al.,* 2001; 2010], experimental results [Noble *et al,* 2007] and modeling [Lucey and Noble, 2008; Lucey and Riner, 2011] demonstrate that nanophase iron-bearing rims and agglutinates both contribute important optical effects, but result from distinctly different combinations of space weathering processes. The small $npFe^0$ in rims causes reddening while the abundant large metal particles in agglutinates result in darkening. We have adopted the terminology “nanophase metallic iron” ($npFe^0$), or more generally, “nanophase opaques” (npOpq) for these very small particles that redden a spectrum and “Britt-Pieters” (B-P) particles (as suggested in Lucey and Noble [2008] and Lucey and Riner [2011]) for the somewhat larger particles that darken without reddening. We propose the term “optically active” opaque particles (OAOpq) to encompass both size ranges.

3 The Debate over Irradiation vs Impact Melt/Vapor Deposition

3.1 Lunar sample and meteorite laboratory studies

The formation mechanisms for the optically active iron in lunar rims and agglutinates has long been debated. Many workers have tried to simulate space weathering in the laboratory by various means. The first such experiments [e.g. Wehner, 1961; Hapke, 1966] irradiated solid surfaces with H ions to reproduce the effects of solar wind, however, no reddening or

darkening was observed. The key, it turned out, was powdered surfaces, and when these were irradiated [e.g. Wehner, 1964; Hapke, 1973] the samples did in fact show substantial reddening and darkening, correlated to the amount of Fe present. These results appeared to suggest that solar wind was a main driver of space weathering. But what role do micrometeoroids play? Moroz *et al* [1996] were the first to use lasers to simulate the effects of micrometeorite bombardment, but the long laser pulse duration (0.5 – 1 μsec) was unrealistic for typical micrometeorite impacts and although the samples did show reddening and darkening, it was thought to be largely due to the rapid melting and recrystallization of the materials. Several researchers [e.g. Yamada *et al.*, 1999; Sasaki *et al.*, 2001, Brunetto *et al.*, 2006; Gillis-Davis *et al.*, 2014; 2015] have successfully used nanosecond pulse lasers, which better reproduce the heating profile, though not the shock, of a micrometeorite impact. TEM analyses of these laser-irradiated analog products show that indeed this process produces optically active iron particles. Figure 5 compares an experimentally laser-irradiated olivine with a natural micrometeorite impact into an olivine grain in a lunar rock. The laser-irradiated olivine in Figure 5 (left) received a single laser shot [Noble *et al.,* 2011]. The $npFe^0$ produced is roughly the same size as is seen in natural impacts [Noble *et al.,* 2016] and in rims on soil grains. Many laser analog experiments however, raster the laser over the surface several times, melting and remelting that surface layer. This seems to also result in the creation of larger iron particles [Sasaki *et al*, 2001; Kurahashi *et al.*, 2002; Rout *et al.*, 2008]. These results are consistent with our understanding of the formation mechanism for the larger B-P particles in agglutinates, because as the small $npFe^0$ in rims is melted and incorporated into agglutinitic glass there is an opportunity for the small iron to coalesce into larger particles.

Another approach is to evaluate the character of rims developed on individual grains with the actual exposure age. By counting the accumulation of solar flare particle tracks, it is now possible to determine the cumulative exposure age of an individual soil grain [Berger and Keller 2015a]. Zhang and Keller [2011] and Keller and Zhang [2015] looked at the thickness of amorphous radiation-damage rims and depositional rims compared to the solar track density. The rim thickness for the radiation-damage rims increases with exposure age as damage accumulates; the depositional rims, in contrast, show no correlation with time. This indicates that creation of the depositional rims is a completely stochastic process and formation of these rims typically happens in a single event, as deposition of vapor and/or melt in an impact, rather than a slow build up via sputtering. Thus, retaining and recycling grains during regolith gardening are important constraints on soil evolution. Both types of rims are roughly equally common in a well developed mature soil [Keller and McKay, 1997]. Both seem to accumulate ~10^6-10^7 yr of integrated exposure in mature lunar soils based on the solar flare track densities in individual space-weathered grains [Keller and Zhang, 2015].

It is clear from the Zhang and Keller [2011] integrated study of natural lunar soil grains that the $npFe^0$ found in lunar soil rims is created largely through impact processes rather than solar wind processes. However, although most experiments mimicking micrometeorite impacts produce $npFe^0$ apparently without the presence of H, it remains unclear if solar wind implantation of H is a necessary precursor to allow for the reduction of iron on the lunar surface.

3.2 Lunar Swirls

It was initially hoped that the special environment found at unusual sinuous albedo features on the Moon, referred to as lunar 'swirls', would provide insight into the character of lunar space weathering. These bright mysterious features contain no topographic relief, and all are associated with local magnetic anomalies (although not all magnetic anomalies found on the Moon are associated with detectible swirls) [Blewett *et al.,* 2011; Denevi *et al,* 2016]. It was commonly hypothesized that the local brightness at swirls was due to protection of the surface from the solar wind by the local magnetic field, resulting in reduced space weathering at these features [e.g., Hood and Schubert, 1980; Hood and Williams, 1989]. Indeed, measurements of swirls with modern sensors detect a deflection of solar wind particles associated with the swirl [Kurata *et al.,* 2005; Wieser *et al.,* 2010; Lue *et al.,* 2011]. Similarly, abundance of the pervasive surficial OH recently detected across the Moon, which is believed to be formed from solar wind H interacting with O-rich surface silicates [Pieters *et al.,* 2009; Sunshine *et al.,* 2009; McCord *et al* 2011], is found to be lower in the bright portion of lunar swirls [Kramer *et al.,* 2011; Pieters *et al.,* 2015], confirming a reduced presence of (solar wind) H at swirls.

Although the local magnetic field at lunar swirls thus appears to protect the surface from exposure to much of solar wind H, modern spectroscopic near-infrared measurements demonstrate that the surface of swirls is not consistent with immature regolith [Pieters *et al.,* 2014]. This significant spectroscopic distinction between normal space weathering trends across fresh craters and that found across lunar swirls is illustrated in Figure 6. The M^3 images cover a flat mare region to the southwest of the main Reiner Gamma swirl. The area contains several small fresh craters, numerous bright and dark markings of swirls, and background mare soil. The bright immature soils associated with small fresh craters are readily recognized in the top image as small localized generally circular bright areas at M^3 visible wavelength. These are easily distinguished from the bright sinuous and diffuse markings of the swirls. However, for the lower near-infrared image at 2200 nm (near the center of a diagnostic pyroxene absorption as illustrated in Figure 2), the immature mare craters largely disappear, but the bright swirls are not affected.

Comparison of the typical maturity trend across a fresh mare crater and surrounding mature soil (Figure 2, right) with the traverse across a bright swirl into a neighboring dark lane (Fig. 6, right) illustrates that the two environments produce entirely different optical effects. In contrast to the prominent pyroxene ferrous absorptions associated with relatively high albedo fresh mare material, the bright swirls exhibit very little difference in absorption band strength compared with dark lanes and nearby mature soils in mare regions, but there is a prominent overall increase in albedo across *all* wavelengths. Although the low OH found at bright regions of mare swirls indicate they are less affected by solar wind H than typical mare soils, their mineralogy has clearly been altered (weak pyroxene absorptions), and the bulk properties of swirls are certainly not comparable to normal immature lunar materials (Fig. 2).

These unusual albedo features and their environment remain shrouded in mystery. It is unknown whether the magnetic environment is sufficiently strong to also deflect heavier energetic particles, and the cause of the general wavelength independent brightening of the

swirl has not been determined. For example, in addition to hypotheses of different soil products formed at swirls due to lower solar wind interactions [e.g. Hemingway *et al.,* 2015], other hypotheses include particle size sorting in a charged-magnetic environment, magnetic sorting of npFe0-bearing and B-P particles during regolith gardening, development of differential rim populations of soil grains, regolith scouring during cometary interaction, etc [Garrick-Bethell *et al.*, 2011; Pieters *et al* 2014, Keller and Zhang, 2015; Syal and Schultz, 2015]. In summary, although clearly associated with local magnetic anomalies (mini-magnetospheres), swirls exhibit their own distinctive optical trends, the cause of which has yet to be determined. They remain some of the most lovely and mysterious features on the lunar surface and certainly merit closer examination in-situ.

4 Space Weathering on Mercury

The environment and composition of Mercury is substantially different from that found on the Moon, and those differences influence how space weathering manifests in the Mercurian regolith. The speed and flux of impactors is substantially greater at Mercury because of its proximity to the Sun and greater mass [Cintala 1992; Marchi *et al.,* 2009]. Per unit area, impacts on Mercury are predicted to produce 13.5 times the melt and 19.5 times the vapor than is produced by similar impacts on the Moon [Cintala, 1992]. Other space weathering processes such as irradiation are also approximately an order of magnitude stronger on Mercury compared with the Moon [Domingue *et al.,* 2014]. Based on Mercury's reflectance spectrum which lacks diagnostic ferrous absorptions (Figure 7), it has long been assumed that Mercury's surface is poor in ferrous iron [McCord and Clark, 1979]. Recent results from MESSENGER have confirmed this and provide additional compositional information about the planet indicating substantially less than 4 wt% Fe across the surface [e.g., Nittler *et al.,* 2011; Evans et al. 2012; Weider *et al.,* 2014]. Furthermore, the composition of the surface was found to be sulfur-rich, with more sulfur than iron. Mercury's regolith is also exposed to an extreme temperature regime. This combination of new compositional information and distinct optical properties associated with fresh craters clearly define the type of space weathering on Mercury seen in Figure 7. Although no ferrous absorptions are present, fresh material exhibits a higher albedo and less steep continuum slope [Robinson *et al* 2008; McClintock *et al* 2008; Blewett *et al* 2009; Izenberg *et al* 2014; Domingue *et al.,* 2014; Murchie *et al* 2015].

Before the arrival of MESSENGER, Noble and Pieters [2003] predicted that due to the higher flux, greater speeds, and higher temperatures, space-weathering products would be created at an accelerated rate on Mercury compared to the Moon. Agglutinates make up a substantial fraction of mature lunar soils (up to 60%); a mature soil on Mercury probably has little original crystalline material remaining. Although there is less iron available, this extreme environment should result in the creation of larger iron/opaque particles as the repeated melting allows small particles to merge with others and coalesce [Noble *et al.*, 2007]. Lucey and Riner [2011] modeled a MESSENGER spectrum, accounting separately for the effects of nanophase and Britt-Pieters particles. Compared to the lunar case, they found the MESSENGER spectrum requires more nanophase as well as Britt-Pieters (opaque) particles, consistent with the higher melt and vapor predicted from micrometeorites [Cintala, 1992]. Unlike the Moon, where only a small percentage of the available iron

(largely FeO) is reduced by space weathering, on Mercury it appears that all, or nearly all, of the endogenic and exogenic available iron is processed. Furthermore, the models of Lucey and Riner [2011] suggest that the ratio of larger Britt-Pieters particles to smaller nanophase particles is significantly higher compared to the lunar case (~6 compared to ~2 for the Moon), consistent with the predictions of Noble and Pieters [2003] and Noble *et al.* [2007].

Even after accounting for both size ranges of optically active iron, modeling suggests that there may be other opaques contributing to the space weathering continuum of Mercury's spectrum, such as nanophase amorphous carbon [Trang *et al.*, 2015]. Impact experiments have demonstrated that carbon-bearing compounds can produce Mercury-like products [Syal *et al.*, 2015] and, indeed, carbon (graphite) is seriously discussed as an ancient crustal component [Vander Kaaden and McCubbin, 2015; Peplowski *et al.*, 2016]. Given the relatively high abundance of surface sulfur discovered by MESSENGER [Nittler *et al.*, 2011; Evans *et al.* 2012], another likely widespread contributor to npOpq and B-P particles on Mercury is a sulfur bearing opaque compound [e.g. Domingue *et al.*, 2014].

The extreme temperature regime at Mercury also appears to play a role in how space weathering manifests. The “hot poles” (equatorial regions at 0 and 180 longitude) experience temperatures up to ~700 K; these regions also appear to be enriched in Britt-Pieters particles. As predicted by Noble and Pieters [2003], the temperatures reached are high enough that the optically active particles can grow through the process of Ostwald ripening [Trang *et al*, 2015].

Although the optical and elemental data now available for Mercury from MESSENGER have certainly provided a more detailed understanding of the character and diversity of the surface, it is also clearly a complex and very harsh space weathering environment. It will likely be a long time before samples are available from Mercury, but inferences and comparisons with the Moon have provided considerable insight. A comprehensive assessment of the special environment at Mercury is presented in the review by Domingue *et al.,* [2014].

5 Space Weathering on Near Earth Asteroids

Any airless body at 1 AU encounters the same space environment conditions as are found at the Moon and Earth. Although still substantial, the uncontrolled variables are reduced to the composition, texture, and mass (gravitational environment) of the host body and the duration of exposure and recycling of particles within the regolith.

5.1 Ordinary Chondrite Bodies

Two near-Earth bodies have been orbited with spacecraft: 433 Eros with the NEAR spacecraft [Cheng, 2002] and 25143 Itokawa with the Hayabusa spacecraft [Tsuchiyama et al., 2014]. Both are classified as an S-type asteroid, and have been shown to be of ordinary-chondrite composition [Trombka *et al.*, 2000; McCoy *et al.*, 2001; Nakamura *et al.,* 2011]. Though similar in composition and elongate shape, they are quite different in scale: Eros has a mean diameter of 16 km, while Itokawa has a mean diameter of just 0.324 km (Figure 8). Both bodies have smooth regions or “ponds” where it appears that fine grained material has

gathered in areas with low geopotential due to several possible mechanisms [Robinson *et al.,* 2001; Cheng *et al.* 2002; Dombard *et al.,* 2010; see review by Roberts *et al.*, 2014]. The ponds on Eros are local features, often in crater bottoms. On Itokawa the "ponding" is a global-scale process but mainly concentrated in two areas: the northern polar region and around the southern polar region including the Muses Sea. These smooth terrains cover roughly 20% of the total surface area of Itokawa [Yano *et al.*, 2006]. Close up images from Hayabusa indicate that the Itokawa ponds consist of mostly gravel-sized (millimeter-centimeter) grains [Yano *et al.,* 2006].

Global spectra mapping of these bodies indicates that space weathering is taking place. On both bodies, fresh bright materials are observed in regions of steep topographic slopes and craters. On Eros there is a strong albedo effect (contrasts up to 40%), but only very minor color differences (4-8% reddening variations) [Clark *et al.*, 2001]. Weathering on Eros seems to follow a different trend than was seen at Gaspra and Ida in the main asteroid belt (see section 6.1 below), where albedo effects are of the same order as spectral reddening and weakening of absorption bands. Although Gaffey [2010] focuses on a potential ambiguity produced by space weathering, Chapman [2004] discussed the possible reasons for this and concluded that it was likely because Eros is a large near Earth asteroid, and therefore exposed to a different space environment. However, weathering trends on Itokawa do not seem to share the extreme albedo effect, but rather show small color and albedo trends similar to those seen at Gaspra and Ida [Hiroi *et al.*, 2006]. Thus, it seems that Eros is the odd one and there must be some environmental or compositional factor controlling the weathering process on Eros that we do not yet understand.

Space weathering has largely been considered to be a soil process, but rocks exposed for extended periods will also incur the effects of space weathering. Weathering patinas on lunar rocks have been described [Wentworth *et al.*, 1999; Noble *et al.*, 2012] but in the lunar case, mature outcrops are only small contributors to the spectrum on a remote sensing scale. Results from the Hayabusa spacecraft at the asteroid Itokawa (Figure 9) suggest that while low gravity does not allow for the development of a mature regolith, weathering patinas can, and do, develop on rock surfaces [Ishiguro *et al.*, 2007]. It is the boulder-rich areas on Itokawa that appear the most weathered, with lower albedos and shallower 1-μm bands [Abe *et al.*, 2006]. The rocks of Eros also appear to be notably dark and space weathered [Chapman, 2004]. For small bodies, where there is little soil and a substantial fraction of the exposed surface is rocky, rock weathering may be an important process.

Although there is no shortage of ordinary chondrite material on Earth, the samples returned from Itokawa were the first opportunity to study true asteroidal regolith samples from a known asteroid in a laboratory. Despite Itokawa's small size and the difficulty of developing a substantial fine-grained regolith, the Hayabusa mission was able to return hundreds of regolith grains from the Muses Sea region [Yano *et al.,* 2006]. Because of the small quantity of available sample, most individual studies have been limited to looking at a handful of grains, making statistical statements difficult. However, space weathering products have been clearly identified on many grains [Noguchi *et al.,* 2011]. The results not only definitively confirm the link between OCs and S-type asteroids [Nakamura *et al.,* 2011], but give us insight into space weathering and regolith processes products on small bodies.

At least two kinds of lunar-like weathering products have been identified on Itokawa grains: vapor deposits and solar wind irradiation effects [Noguchi *et al.,* 2011]. However, the vapor-deposited material found on Itokawa grains is thin (5-15 nm) and contains nanophase opaques (npOpq) that contain sulfur, not just iron. Sulfur-free $npFe^0$ particles exist deeper inside (up to 60 nanometers) some of the iron-bearing silicates where Fe^{2+} is reduced in-situ, creating $npFe^0$ particles in solar wind amorphous rims, a process occasionally seen in lunar soils as well, particularly in olivine [Berger and Keller, 2015b]. Both processes on Itokawa create small nanophase opaques (~2 nm), similar in size to that seen in rims of lunar grains.

Berger and Keller [2015b] found that the two grains they examined had been buried in a relatively fixed orientation at depths of a few millimeters to a few centimeters for $\sim 10^4$-10^5 yrs, based on solar flare track gradients. The solar wind damage rims, on the other hand, indicate that late in their history ($<10^3$ yrs), they were brought to the surface and the continuous nature of those rims suggests they must have moved to expose all sides. Furthermore, unlike the sharp angles of lunar soil grains, some of the Itokawa grains have rounded edges, possibly due to to abrasion from seismic-induced grain motion [Tsuchiyama *et al.,* 2011]. Taken together, this suggests that there is little deep overturn/gardening on Itokawa, but the grains at the uppermost surface move about frequently.

5.2 Carbonaceous Chondrite (primitive) Bodies

Analysis of the regolith grains returned from Itokawa by Hayabusa [Noguchi *et al.,* 2011; Nakamura *et al.,* 2011] provided critical information demonstrating that lunar-like optically active nanophase opaques are produced in the environment of an ordinary chondrite parent body. Such space weathering products occurs for these S-type asteroids that contain silicates lithologies consisting of mafic minerals (pyroxene, olivine) as well as Fe-Ni metal and FeS. However, another major class of near-Earth asteroids fall into the C-type class, which are dark and without distinguishing diagnostic absorption bands. It is generally thought that these objects have affinities to the carbonaceous chondrite (CC) class of meteorites that fall to Earth, although no direct link has been made. These CC meteorites are very primitive and typically contain carbon compounds, organics, and hydrous minerals. If they are derived from C-type asteroids, then their distinctive composition is completely different from all the anhydrous materials studied from the Moon and OC parent bodies.

A few laser and ion irradiation experiments relevant to space weathering have been performed with CC meteorites [Moroz *et al,* 2004; Gillis Davis *et al.,* 2015; Kaluna *et al.,* 2015; Lantz *et al.,* 2015; Matsuoka *et al.,* 2015] to determine whether products are formed that can be interpreted to result from the space weathering context involving micrometeoroid impact or solar wind interaction. The experimental results have provided highly diverse products, however, and no regular pattern has been detected across samples. From the experiments, it appears the mineralogy itself has often been readily altered and new and/or additional alteration products are formed for CC-like primitive materials that are specific to the starting composition of the particular parent body.

Fortunately, it is expected that two missions, Hayabusa 2 (JAXA) and OSIRIS-REx (NASA), traveling to two different small C-type near-Earth asteroids will be returning samples from

the surface of these asteroids to Earth-based laboratories in the not too distant future. We are not going to make predictions about what form of space weathering processes and products might be found, other than these unique asteroid regolith samples are likely to surprise us with something completely new.

6 Space Weathering on Main Belt Asteroids

6.1 Gaspra and Ida

The Galileo flybys of Gaspra and Ida provided the first close-up views of the surface of asteroids. Both are S-type asteroids similar to Eros and both show evidence of “lunar-style” space weathering, i.e. a reddened continuum slope and weaker absorption bands compared to the spectra of fresh craters [Chapman, 1996]. The changes are more subtle at Gaspra, which corresponds to the relatively fewer large craters compared to Ida and suggests that Gaspra's surface is younger. Appearing even less weathered is Dactyl, Ida's tiny moon, which is too small to retain a regolith. Extrapolating the spectral trend from weathered-Ida to fresh-Ida to Dactyl points towards the spectra of ordinary chondrites (OCs), as illustrated in Figure 10. This trend provided the first direct link between OCs and S-IV asteroids, thus pointing to space weathering as the likely answer to the “S-type conundrum”.

6.2 Vesta

The spectrum of asteroid Vesta was one of the first measured for an asteroid using Earth-based spectrophotometry [McCord *et al.*, 1970]. Diagnostic absorption features identified the presence of low-Ca pyroxene and showed the asteroid to have a clear affinity to the HED class of differentiated meteorites (Howardite, Eucrite, Diogenite). This Vesta-HED association was only strengthened as measurements improved [McFadden *et al.*, 1977; Binzel and Xu 1993; Gaffey, 1997] and was confirmed with the detailed data acquired by the Dawn mission at Vesta [De Sanctis, *et al.* 2012a]. However, unlike the Moon and near-Earth asteroids, the overall surface of Vesta was able to be directly compared to particulate meteorites prepared to small particle sizes [e.g. Hiroi *et al.*, 1994], and no space weathering effects were necessarily required to fit the lab spectra to the remote observations. This was the conundrum that puzzled the community [Chapman 2004], namely how can highly space weathered bodies like the Moon, Mercury, and some asteroids co-exist with a prominent asteroid that does not exhibit the distinctive ‘reddening’ associated with exposure to the space environment?

The answer became apparent when Vesta was visited by the Dawn spacecraft, and its physical properties and local mineralogy were measured with modern sensors [e.g., Russell *et al.*, 2013]. Like other silicate bodies, Vesta does contain both fresh and degraded craters, with the fresh craters commonly exhibiting rays of material emanating from the crater resulting in deposits on or disruptions to the surrounding environment (Figure 11). Again, like on other bodies, these rays degrade and disappear with time indicating an active space weathering environment. Although the strength of diagnostic ferrous absorption features was found to decrease a little with increasing development of soil with properties comparable to the background, no change of the near-infrared continuum was observed in local spectra [Pieters *et al.*, 2012]. Independent parallel measurements detected small but distinct amounts

of H or OH in a spatially coherent pattern across Vesta [Prettyman *et al.*, 2012; De Sanctis *et al.*, 2012b]. This pattern is not correlated with latitude (as on the Moon) but instead is spatially anti-correlated with albedo. Since the average impact velocity within the main asteroid belt is substantially lower than that found for the Moon, the preferred interpretation is that the origin of OH on Vesta is exogenic, and specifically linked to surface contamination with dark water-rich carbonaceous chondrites. A detailed examination of Vesta terrains with differing mineralogies [Blewett *et al.,* 2016] failed to detect spectral effects that could be attributed to accumulation of $npFe^0$, and in all cases regolith evolution appears to be closely tied to admixture of exogenic carbonaceous chondrite material. Thus, the integrated interpretation is that space weathering on Vesta is not dominated by the development of nanophase opaques as on the Moon and Mercury and instead is principally the result of regolith mixing with micrometeorites dominated by carbonaceous chondrite-like material [Pieters *et al.,* 2012]. The lack of development of abundant $npFe^0$ on Vesta can be attributed to multiple environmental and mineralogical factors that are specific to Vesta.

The most likely reason Vesta does not exhibit measurable lunar-like $npFe^0$ space weathering products is a combination of its physical environment (lower solar flux and less energetic micrometeoroids) and, more importantly for that environment, its total lack of metallic iron or sulfides that can be mobilized to produce npOpq. In contrast, even though Mercury has very low iron content, it is located in an intense micrometeorite and solar irradiance environment and has high sulfur content to combine with other elements to produce abundant npOpq as well as B-P particles and hence exhibits extensive lunar-like space weathering. Vesta's neighboring S-type asteroids across the main belt that exhibit modest lunar-like space weathering (although considerably less than the Moon) are presumed to be of an ordinary chondrite-like composition and thus have abundant metallic iron and FeS that can be readily mobilized to produce the npOpq. It is largely Vesta's unusual differentiated metal-free basaltic composition in the asteroid belt that allows it to retain its more pristine mineral appearance over billions of years' exposure.

6.3 Ceres

Ceres is the largest and most massive asteroid in the main asteroid belt, and its spherical shape leads it to be classified as a dwarf planet. Ceres' low density (2.16 g/c) and recently measured gravity harmonics [Park *et al.,* 2016] confirm it is volatile-rich and experienced some amount of physical and chemical differentiation during its early evolution (Russell et al., 2016). Ceres is thus a transitional body between the rocky bodies of the inner solar system and the ice-rich bodies of the outer solar system. It exhibits a mineralogy not encountered elsewhere and is not represented in the meteorite collection [De Sanctis *et al.,* 2015; Ammannito *et al* 2016]. The overall surface is very dark, and color variations across the visible are only a few percent [Nathues *et al.,* 2015]. Spectral ratio images (illustrated in Figure 12) are required to map and evaluate subtle spatial variations of color. A few small locations are distinctly bright, such as the unusual areas in the center of Occator crater [Russell *et al.,* 2016] which have reflectance 5-8× greater than surrounding material [Li *et al.,* 2016].

Fresh craters on Ceres (and surrounding ray system when they exist) exhibit distinct optical properties but these features evolve into background material with time. As Dawn data for Ceres are evaluated, it is clear that a different group of space weathering processes dominate the surface of Ceres compared with those for previously studied bodies. This is most likely related to Ceres' location in the main asteroid belt, and (more importantly) to the inherent compositional character and evolution of its surface. The development of lunar-like anhydrous space weathering npOpq products is likely to be unimportant for volatile-rich Ceres, where large impact craters excavate and distribute volatile-rich materials and hydrated minerals from depth. However, water ice is not stable on the surface of Ceres [Fanale and Salvail, 1989] and will be lost with time, leaving non-volatile materials behind. These can consist of salts (including carbonates) previously dissolved in aqueous sub-surface materials, as well as a variety of endogenic hydrated minerals and exogenic contaminants. The hypothesis being tested with Dawn data [e.g., Pieters *et al.*, 2016] is that the overall dark surface results from a lag deposit developed over billions of years and that the “blue” large young craters and rays contain a component of residual salts deposited on the surface that have not yet been completely mixed into the background regolith. The processes most likely to be actively involved in space weathering on Ceres are summarized in Figure 13.

7 Space Weathering on the Moons of Mars

The two moons of Mars, Phobos and Deimos, are some of the most enigmatic of airless bodies. They have been measured by sensors on Earth-based telescopes as well as on multiple spacecraft sent to the Mars environs. Since most spacecraft are located closer to Mars than Phobos' orbit, it is the Mars-facing side of Phobos that is most often observed. Although Phobos is better studied than Deimos, data are severely limited in surface coverage, as well as spatial and spectral resolution provided by available sensors. We thus know less about these moons than we do for many of the other small bodies that have been visited by spacecraft. A major unsolved question is whether these small moons (D_{Phobos}=22.2 km, D_{Deimos}=12.6 km) are captured asteroids or are directly related to Mars by accretion of Mars debris resulting from a major impact and subsequently space weathered in situ [e.g., Rosenblatt 2011].

As can be seen in Figure 14, the present surface of Phobos is not homogeneous. The overall bulk properties could be consistent with either a dark primitive “D-type” asteroid or silicate material of the inner solar system that has been highly, perhaps extremely, space weathered (see data summary in Rivkin *et al.*, 2002; Fraeman *et al.*, 2012; 2014; Pieters *et al.,* 2014). With no obvious diagnostic absorption features readily detected in available visible and near-infrared spectra, the principal variation in optical properties of surface material is largely a distinct difference in continuum slope. In visible wavelength images, regions with a steep (‘red’) continuum are also darker, but albedo variations appear less distinct in the near-infrared. The optical differences observed across Phobos could be due to either inherent heterogeneities of materials comprising the satellite or to variations of how regolith forms or is altered and distributed across the surface. The large crater, Stickney, with substantial ‘blue sloped’ material found on its rim is also on the leading edge of Phobos as it orbits Mars. The satellite is only ~6000 km from the surface of Mars and particles on or near the surface are necessarily affected by the Mars gravity well. Large particles disturbed from the surface are

predicted to eventually re-accrete on Phobos after spending time in Mars orbit, whereas fine particles are swept away toward Mars [Ramsey and Head, 2013; Zakharov *et al.*; 2014]. The regolith on Phobos, and by extension on Deimos, is therefore highly evolved and may be relatively mobile, but the origin of the regolith and the satellites themselves is not yet clear.

8 Discussion and Integration

Space weathering was first encountered as a mystery to solve: why do soils returned from the Moon look so very different than the rocks from which they were derived? Solution of this mystery took decades of multiple investigators probing samples with increasingly sophisticated techniques in the laboratory as well as initiating diverse experiments and modeling in order to converge on an understanding of the dominant processes and products involved [e.g., Pieters *et al.*, 2000; Hapke 2001].

Through the integration of studies associated with the Moon, S-type asteroids, and Mercury, it is now clear that several common forms of space weathering produce small opaque particles that darken the surface and control its optical properties. It is the size and abundance of these accumulated particles that is very important in determining the optical effects. Since our understanding of this opaque component of observed space weathering products has evolved considerably over the last few decades as documented above, we recommend the following terminology be used to describe opaque or absorbing particles in order to be consistent and avoid confusion:

A. **Nanophase metallic iron (npFe^0) or other nanophase opaque (npOpq) particles.** These are typically in the size range of 1-15 nm and accumulate on/in the rims of individual regolith grains imparting a red-sloped continuum in the visible to near-infrared. At low abundances, these particles affect the shorter wavelengths more strongly resulting in a curved continuum.

B. **Britt-Pieters (B-P) opaque particles (Fe^0, FeS, etc).** These are in the size range from ~40 nm to 2 μm (commonly termed microphase) and are dispersed throughout the matrix of larger particles through impact and friction processes or accumulate in complex glass-welded soil components (agglutinates) produced during repeated small impacts or heating events. Opaque particles of these sizes impose a strongly absorbing (darkening) effect with little or no wavelength dependence.

C. **Optically active opaque (OAOpq) particles** These can include both npOpq and B-P particles as well as any group of dark or opaque particles of poorly characterized or undetermined properties. In short, this term can be used when the physical form of absorbing material is simply not known.

On a related matter, it should be noted that optically active opaque (OAOpq) particles are an inherent component in what many lunar petrologists simply call ‘glass’, or amorphous optically dense material with no easily-defined mineral components that often occurs in breccias or impact melt. When referring to ‘glass’ we strongly recommend adjectives also be used to define the actual type of material discussed. Quench glass in particular has distinctive and readily recognized optical properties [Bell *et al,* 1976], but such a material is

not often found in lunar samples by optical techniques [e.g. Tompkins and Pieters, 2010]. Concentrations of quench glass principally occur as products of rapidly cooled pyroclastic volcanism such as orange glass 74220 and green glass 15401. The more common messy dark amorphous glass of lunar impact melt and breccias (see Tompkins and Pieters [2010] examples), can take on a range of optical properties depending on the actual character of its sub-microscopic components which are almost never well characterized. In some cases the 'glass' can be fully crystalline but at such a small scale to be unrecognized by most techniques. In other situations (perhaps most), the amorphous material is an unresolved mixture of npOpq and B-P particles intimately intermixed with crystalline material of a similar small size plus various amounts of residual uncrystallized glass. The bulk geochemical properties of such common dark amorphous material can readily be measured analytically, but its mineralogy (and consequently optical properties) is undetermined. Unraveling the complex composition and history of breccias and various forms of impact melt remains an important challenge to analytical techniques in the years ahead.

A key aspect of being able to detect alteration effects of space weathering processes is the ability of the regolith to accumulate and retain the space weathering products. All things being equal for a specific surface, a key variable is of course the time since the surface was formed. Also important, however, is the ability of the surface to retain and recycle a regolith that accumulates alteration products. This distinction is readily recognized in the lunar case where steep topographic slopes of older craters or prominent mountains/massifs are unable to collect a well developed soil. These areas exhibit properties of an immature regolith whereas nearby topographically flat areas with the same formation age exhibit well developed or mature regolith. In a similar manner, small bodies with low mass are expected to be less able to retain and recycle regolith than larger bodies of the same composition and consequently small bodies accumulate less space weathering effects. For example, this was well illustrated with small S-type near-Earth asteroids < 5 km in size [Binzel *et al.*, 2004].

Altogether, much has been learned about space weathering processes and products since the first return of samples from an airless planetary body. The lunar framework for understanding the magnitude and extent of space weathering products is now known to involve accumulation of optically active opaques. This framework has met with reasonable success for understanding other solar system rocky bodies that are composed largely of anhydrous materials such as Mercury and some asteroids (S-type). However, in situations where an environment is able to only produce minimal OAOpq space weathering products (such as at Vesta), exogenic contamination and regolith mixing become the dominant processes of gradually altering optical properties of the regolith. This recognition that cross-contamination among solar system bodies can often significantly affect the measured properties of surface material is an important lesson to highlight as we further explore solid bodies of the solar system.

On the other hand, documenting and identifying space weathering products and the alteration processes involved for surfaces of hydrous or volatile-rich bodies is much less understood. For most solid bodies we can only study the exposed surface with advanced remote sensing tools and model or constrain the observations with available laboratory experiments. We have initial observations of the presence of space weathering at Ceres and

several hypotheses to test its origin. We recognize a diverse and extensive range of dark asteroids that are likely to contain a plethora of altered hydrous minerals or organic components, but their surfaces are not yet well explored. A wide range of volatile-rich or icy bodies exist, encompassing comets (and their offspring), Ceres, a multitude of satellites in the outer solar system, and even Pluto. As samples are returned from two dark (and presumed primitive) asteroids by Hayabusa-2 and OSIRIS-REx and increasingly sophisticated laboratory experiments are pursued, the next several decades of space weathering research will certainly clarify and expand our understanding of the mysteries and challenges that space weathering has placed before us across diverse conditions of the natural environment.

Acknowledgments

Data for this paper are properly cited and specific files are identified in figure captions and can be found through the references identified or PDS. RELAB data can be found through http://www.planetary.brown.edu/relabdocs/relab.htm. We especially thank Lindsay Keller for contributing new TEM image (Figure 3b). The comments and suggestions by David Blewett and Paul Lucey were much appreciated and strengthened the final manuscript. This work has been supported through a NASA SSERVI cooperative agreement NNA14AB01A.

References

Abe M, et al. Near-infrared spectral results of asteroid Itokawa from the Hayabusa spacecraft. Science. 2006; 312(5778):1334–1338. DOI: 10.1126/science.1125718 [PubMed: 16741108]

Adams J, McCord T. Remote sensing of lunar surface Mineralogy: Implications from visible and near-infrared reflectivity of Apollo 11 samples. Geochim & Cosmochim Acta Supp, Proc Apollo 11 Lunar Sci Conf. 1970; 3:1937–1945.

Ammannito E, et al. Distribution of Phyllosilicates on the surface of Ceres. Science. 2016 In Press.

Bell, JF., Davis, DR., Hartmann, WK., Gaffey, MJ. Asteroids-The big picture, in *Asteroids II*. Gehrels, T., editor. The University of Arizona Press; 1989. p. 921-945.

Bell PM, Mao HK, Weeks RA. Optical spectra and electron paramagnetic resonance of lunar and synthetic glasses - A study of the effects of controlled atmosphere, composition, and temperature. Proc Lunar Sci Conf, 7th. 1976:2543–2559.

Berger, EL., Keller, LP. Lunar Planet Sci. The Woodlands, TX: 2015a. Solar Flare Track Exposure Ages in Regolith Particles: A Calibration for Transmission Electron Microscope Measurements; p. 46-1543.

Berger, EL., Keller, LP. Lunar Planet Sci. The Woodlands, TX: 2015b. Space Weathering of Itokawa Particles: Implications for Regolith Evolution; p. 46-2351.

Binzel RP, Xu S. Chips off of Asteroid 4 Vesta: Evidence for the Parent Body of Basaltic Achondrite Meteorites. Science. 1993; 260(5105):186–191. DOI: 10.1126/science.260.5105.186 [PubMed: 17807177]

Binzel RP, Rivkin AS, Stuart JS, Harris AW, Bus SJ, Burbine TH. Observed spectral properties of near-Earth objects: results for population distribution, source regions, and space weathering processes. Icarus. 2004; 170(2):259–294. DOI: 10.1016/j.icarcus.2004.04.004

Blewett DT, Robinson MS, Denevi BW, Gillis-Davis JJ, Head JW, Solomon SC, Holsclaw GM, McClintock WE. Multispectral images of Mercury from the first MESSENGER flyby: Analysis of global and regional color trends. Earth Planet Sc Lett. 2009; 285(3-4):272–282. DOI: 10.1016/j.epsl.2009.02.021

Blewett DT, Coman EI, Hawke B, Gillis-Davis JJ, Purucker ME, Hughes CG. Lunar swirls: Examining crustal magnetic anomalies and space weathering trends. Journal of Geophysical Research: Planets. 2011; 116(E2)doi: 10.1029/2010JE003656

Blewett DT, et al. Optical space weathering on Vesta: Radiative-transfer models and Dawn observations. Icarus. 2016; 265:161–174. DOI: 10.1016/j.icarus.2015.10.012

Britt DT, Pieters CM. Darkening in Black and Gas-Rich Ordinary Chondrites - the Spectral Effects of Opaque Morphology and Distribution. Geochim Cosmochim Ac. 1994; 58(18):3905–3919. DOI: 10.1016/0016-7037(94)90370-0

Cassidy W, Hapke B. Effects of darkening processes on surfaces of airless bodies. Icarus. 1975; 25:371–383.

Chapman CR. S-type asteroids, ordinary chondrites, and space weathering: The evidence from Galileo's fly-bys of Gaspra and Ida. Meteorit Planet Sci. 1996; 31(6):699–725.

Chapman CR. Space weathering of asteroid surfaces. Annual Review of Earth and Planetary Sciences. 2004; 32(1):539–567. DOI: 10.1146/annurev.earth.32.101802.120453

Cheng, AF. Near Earth Asteroid Rendezvous: Mission Summary in *Asteroids III*. Bottke, WF., editor. The University of Arizona Press; 2002. p. 351-366.

Cheng AF, Izenberg N, Chapman CR, Zuber MT. Ponded deposits on asteroid 433 Eros. Meteorit Planet Sci. 2002; 37(8):1095–1105. DOI: 10.1111/j.1945-5100.2002.tb00880.x

Cintala MJ. Impact-induced thermal effects in the lunar and Mercurian regoliths. Journal of Geophysical Research. 1992; 97(E1):947–973. DOI: 10.1029/91JE02207

Clark BE, et al. Space weathering on Eros: Constraints from albedo and spectral measurements of Psyche crater. Meteorit Planet Sci. 2001; 36(12):1617–1637. DOI: 10.1111/j.1945-5100.2001.tb01853.x

De Sanctis MC, et al. Spectroscopic Characterization of Mineralogy and Its Diversity Across Vesta. Science. 2012a; 336(6082):697–700. DOI: 10.1126/Science.1219270 [PubMed: 22582257]

De Sanctis MC, et al. Detection of Widespread Hydrated Materials on Vesta by the Vir Imaging Spectrometer on Board the Dawn Mission. Astrophys J Lett. 2012b; 758(2)doi: 10.1088/2041-8205/758/2/L36

De Sanctis MC, et al. Ammoniated phyllosilicates with a likely outer Solar System origin on (1) Ceres. Nature. 2015; 528(7581):241–244. DOI: 10.1038/nature16172 [PubMed: 26659184]

Denevi BW, Robinson MS, Boyd AK, Blewett DT, Klima RL. The distribution and extent of lunar swirls. Icarus. 2016; 273:53–67. DOI: 10.1016/j.icarus.2016.01.017

Dombard AJ, Barnouin OS, Prockter LM, Thomas PC. Boulders and ponds on the Asteroid 433 Eros. Icarus. 2010; 210(2):713–721. DOI: 10.1016/j.icarus.2010.07.006

Domingue DL, et al. Mercury's Weather-Beaten Surface: Understanding Mercury in the Context of Lunar and Asteroidal Space Weathering Studies. Space Sci Rev. 2014; 181(1-4):121–214. DOI: 10.1007/S11214-014-0039-5

Evans LG, et al. Major-element abundances on the surface of Mercury: Results from the MESSENGER Gamma-Ray Spectrometer. Journal of Geophysical Research: Planets. 2012; 117(E12):n/a–n/a. DOI: 10.1029/2012JE004178

Fanale FP, Salvail JR. The water regime of asteroid (1) Ceres. Icarus. 1989; 82(1):97–110. DOI: 10.1016/0019-1035(89)90026-2

Fraeman AA, et al. Analysis of disk-resolved OMEGA and CRISM spectral observations of Phobos and Deimos. Journal of Geophysical Research: Planets. 2012; 117(E11):n/a–n/a. DOI: 10.1029/2012JE004137

Fraeman AA, Murchie SL, Arvidson RE, Clark RN, Morris RV, Rivkin AS, Vilas F. Spectral absorptions on Phobos and Deimos in the visible/near infrared wavelengths and their compositional constraints. Icarus. 2014; 229:196–205. DOI: 10.1016/j.icarus.2013.11.021

Gaffey MJ. Surface Lithologic Heterogeneity of Asteroid 4 Vesta. Icarus. 1997; 127(1):130–157. DOI: 10.1006/icar.1997.5680

Gaffey MJ. Space weathering and the interpretation of asteroid reflectance spectra. Icarus. 2010:564–574.

Garrick-Bethell I, Head JW, Pieters CM. Spectral properties, magnetic fields, and dust transport at lunar swirls. Icarus. 2011; 212(2):480–492. DOI: 10.1016/J.Icarus.2010.11.036

Gillis-Davis, JJ., Scott, ERD. Explaining the Sulfur Depletion on Eros and the Different Space Weathering of S-Type and V-Type Asteroids. 45th Lunar and Planetary Science Conference; Abstract #1189, Lunar and Planetary Institute, Houston. 2014.

Gillis-Davis, JJ., Gasda, PJ., Bradley, JP., Ishii, HA., Bussey, DBJ. Laser Space Weathering of Allende (CV2) and Murchison (CM2) Carbonaceous Chondrites. 46th Lunar and Planetary Science Conference; Abstract #1607, Lunar and Planetary Institute, Houston. 2015.

Gold T. The lunar surface. Mon Not R Astron Soc. 1955; 115:585–604.

Hapke, B. Optical properties of the Moon's surface. In: Hess, W.Menzel, D., O'Keefe, J., editors. The Nature of the Lunar Surface. Johns Hopkins Press; Baltimore: 1966. p. 141-154.

Hapke B. Darkening of silicate rock powders by solar wind sputtering. The Moon. 1973; 7:342.doi: 10.1007/BF00564639

Hapke B. Bidirectional spectroscopy. 1. Theory. J Geophys Res. 1981; 86:3039–3054.

Hapke, B. Theory of Reflectance and Emittance Spectroscopy. Cambridge Univ. Press; New York: 1993.

Hapke B. Space weathering from Mercury to the asteroid belt. Journal of Geophysical Research. 2001; 106(E5):10039–10073. DOI: 10.1029/2000JE001338

Hemingway DJ, Garrick-Bethell I, Kreslavsky MA. Latitudinal variation in spectral properties of the lunar maria and implications for space weathering. Icarus. 2015; 261:66–79. DOI: 10.1016/j.icarus.2015.08.004

Hiroi T, Abe M, Kitazato K, Abe S, Clark BE, Sasaki S, Ishiguro M, Barnouin-Jha OS. Developing space weathering on the asteroid 25143 Itokawa. Nature. 2006; 443(7107):56–58. DOI: 10.1038/nature05073 [PubMed: 16957724]

Hiroi T, Pieters CM, Takeda H. Grain-Size of the Surface Regolith of Asteroid 4 Vesta Estimated from Its Reflectance Spectrum in Comparison with HED Meteorites. Meteoritics. 1994; 29(3):394–396.

Hood L, Williams C. The lunar swirls-Distribution and possible origins. 19th Lunar and Planetary Science Conference Proceedings. 1989:99–113.

Hood LL, Schubert G. Lunar Magnetic Anomalies and Surface Optical Properties. Science. 1980; 208(4439):49–51. DOI: 10.1126/science.208.4439.49 [PubMed: 17731569]

Izenberg NR, et al. The low-iron, reduced surface of Mercury as seen in spectral reflectance by MESSENGER. Icarus. 2014; 228:364–374. DOI: 10.1016/J.Icarus.2013.10.023

Kaluna, HM., Gillis-Davis, JJ., Lucey, PG., Masiero, JR., Meech, KJ. Workshop on Space Weathering of Airless Bodies: Integration of Remote Sensing Data, Laboratory Experiments, and Sample Analysis. Lunar and Planetary Institute; Houston: 2015. Space Weathering Trends Among Carbonaceous Asteroids and Materials. Abstract #2009

Keller, LP., Clemett, SJ. Formation of nanophase iron in the lunar regolith. 32nd Lunar and Planetary Science Conference; Abstract #2097, Lunar and Planetary Institute, Houston. 2001.

Keller LP, McKay DS. Discovery of Vapor Deposits in the Lunar Regolith. Science. 1993; 261(5126): 1305–1307. DOI: 10.1126/science.261.5126.1305 [PubMed: 17731858]

Keller LP, McKay DS. The nature and origin of rims on lunar soil grains. Geochim Cosmochim Ac. 1997; 61(11):2331–2341. DOI: 10.1016/S0016-7037(97)00085-9

Keller, LP., Zhang, S. Workshop on Space Weathering of Airless Bodies: Integration of Remote Sensing Data, Laboratory Experiments, and Sample Analysis. Abstract #2056, Lunar and Planetary Institute; Houston: 2015. Rates of Space Weathering in Lunar Soils.

Kramer GY, et al. M-3 spectral analysis of lunar swirls and the link between optical maturation and surface hydroxyl formation at magnetic anomalies. J Geophys Res-Planet. 2011; :116.doi: 10.1029/2010je003729

Kurahashi E, Yamanaka C, Nakamura K, Sasaki S. Laboratory simulation of space weathering: ESR measurements of nanophase metallic iron in laser-irradiated materials. Earth, Planets and Space. 2002; 54(12):e5–e7. DOI: 10.1186/bf03352448

Kurata M, Tsunakawa H, Saito Y, Shibuya H, Matsushima M, Shimizu H. Mini-magnetosphere over the Reiner Gamma magnetic anomaly region on the Moon. Geophysical Research Letters. 2005; 32(24)doi: 10.1029/2005GL024097

Lantz C, Brunetto R, Barucci MA, Dartois E, Duprat J, Engrand C, Godard M, Ledu D, Quirico E. Ion irradiation of the Murchison meteorite: Visible to mid-infrared spectroscopic results. Astron & Astroph. 2015; 577:A41.doi: 10.1051/0004-6361/201425398

Li, Jian-Yang, et al. Surface Albedo and Spectral Variability of Ceres. The Astrophysical Journal Letters. 2016; 817(2):L22.doi: 10.3847/2041-8205/817/2/L22

Lucey PG, Blewett DT, Taylor GJ, Hawke BR. Imaging of lunar surface maturity. J Geophys Res. 2000; 105:E8, 20377–20386.

Lucey PG, Noble SK. Experimental test of a radiative transfer model of the optical effects of space weathering. Icarus. 2008; 197(1):348–353. DOI: 10.1016/j.icarus.2008.05.008

Lucey PG, Riner MA. The optical effects of small iron particles that darken but do not redden: Evidence of intense space weathering on Mercury. Icarus. 2011; 212(2):451–462. DOI: 10.1016/j.icarus.2011.01.022

Lue C, Futaana Y, Barabash S, Wieser M, Holmstrom M, Bhardwaj A, Dhanya MB, Wurz P. Strong influence of lunar crustal fields on the solar wind flow. Geophysical Research Letters. 2011; 38doi: 10.1029/2010GL046215

Matsuoka M, Nakamura T, Kimura Y, Hiroi T, Nakamura R, Okumura S, Sasaki S. Pulse-laser irradiation experiments of Murchison CM2 chondrite for reproducing space weathering on C-type asteroids. Icarus. 2015; 254:135–143. DOI: 10.1016/j.icarus.2015.02.029

McClintock WE, et al. Spectroscopic observations of Mercury's surface reflectance during MESSENGER's first mercury flyby. Science. 2008; 321(5885):62–65. DOI: 10.1126/Science.1159933 [PubMed: 18599769]

McCord TB, Adams JB, Johnson TV. Asteroid Vesta: Spectral Reflectivity and Compositional Implications. Science. 1970; 168(3938):1445–1447. DOI: 10.1126/science.168.3938.1445 [PubMed: 17731590]

McCord TB, Clark RN. The Mercury soil: Presence of Fe^{2+} J Geophys Res. 1979; 84:7664–7668.

McCord TB, Taylor LA, Combe JP, Kramer G, Pieters CM, Sunshine JM, Clark RN. Sources and physical processes responsible for OH/H2O in the lunar soil as revealed by the Moon Mineralogy Mapper (M-3). J Geophys Res-Planet. 2011; :116.doi: 10.1029/2010je003711

McCoy TJ, et al. The composition of 433 Eros: A mineralogical-chemical synthesis. Meteorit Planet Sci. 2001; 36:1661–1672.

McFadden LA, McCord TB, Pieters C. Vesta: The first pyroxene band from new spectroscopic measurements. Icarus. 1977; 31(4):439–446. DOI: 10.1016/0019-1035(77)90147-6

Moroz LV, Fisenko AV, Semjonova LF, Pieters CM, Korotaeva NN. Optical effects of regolith processes on S-asteroids as simulated by laser shots on ordinary chondrite and other mafic materials. Icarus. 1996; 122:366–382.

Moroz, LV., Hiroi, T., Shingareva, TV., Basilevsky, AT., Fisenko, AV., Semjonova, LF., Pieters, CM. Reflectance Spectra of CM2 Chondrite Mighei Irradiated with Pulsed Laser and Implications for Low-Albedo Asteroids and Martian Moons. 35th Lunar and Planetary Science Conference; Abstract #1279, Lunar and Planetary Institute, Houston. 2004.

Morris RV. Surface exposure indices of lunar soils: A comparative FMR study. Proc Lunar Planet Sci Conf 7^{th}. 1976:315–335.

Morris RV. The surface exposure (maturity) of lunar soils: Some concepts and I_s/FeO compilation. Proc Lunar Planet Sci Conf 9^{th}. 1978:2287–2297.

Murchie SL, et al. Orbital multispectral mapping of Mercury with the MESSENGER Mercury Dual Imaging System: Evidence for the origins of plains units and low-reflectance material. Icarus. 2015; 254:287–305. DOI: 10.1016/j.icarus.2015.03.027

Nakamura T, et al. Itokawa Dust Particles: A Direct Link Between S-Type Asteroids and Ordinary Chondrites. Science. 2011; 333(6046):1113–1116. DOI: 10.1126/science.1207758 [PubMed: 21868667]

Nathues A, et al. Sublimation in bright spots on (1) Ceres. Nature. 2015; 528(7581):237–240. DOI: 10.1038/nature15754 [PubMed: 26659183]

Nittler LR, et al. The Major-Element Composition of Mercury's Surface from MESSENGER X-ray Spectrometry. Science. 2011; 333(6051):1847–1850. DOI: 10.1126/science.1211567 [PubMed: 21960623]

Noble, SK. PhD Thesis. Brown University; 2004. Turning Rock Into Regolith: The Physical and Optical Consequences of Space Weathering in the Inner Solar System.

Noble SK, Pieters CM. Space weathering on Mercury: Implications for remote sensing. Solar System Res. 2003; 37(1):31–35. DOI: 10.1023/A:1022395605024

Noble SK, Pieters CM, Keller LP. An experimental approach to understanding the optical effects of space weathering. Icarus. 2007; 192(2):629–642. DOI: 10.1016/J.Icarus.2007.07.021

Noble SK, Keller LP, Pieters CM. Evidence of space weathering in regolith breccias II: Asteroidal regolith breccias. Meteorit Planet Sci. 2010; 45(12):2007–2015. DOI: 10.1111/J.1945-5100.2010.01151.X

Noble SK, Hiroi T, Keller LP, Rahman Z, Sasaki S, Pieters CM. Experimental space weathering of ordinary chondrites by nanopulse laser: TEM results. 42nd Lunar and Planetary Science Conference. 2011 Abstract #1382.

Noble, SK., Keller, LP., Christoffersen, R., Rahman, Z. Space Weathering of Lunar Rocks. 4rd Lunar and Planetary Science Conference; Abstract #1239, Lunar and Planetary Institute, Houston. 2012.

Noble, SK., Keller, LP., Christoffersen, R., Rahman, Z. The Microstructure of Lunar Micrometeorite Impact Craters. 47th Lunar and Planetary Science Conference; Abstract #1465, Lunar and Planetary Institute, Houston. 2016.

Noguchi T, et al. Incipient Space Weathering Observed on the Surface of Itokawa Dust Particles. Science. 2011; 333(6046):1121–1125. DOI: 10.1126/science.1207794 [PubMed: 21868670]

Park RS, et al. A partially differentiated interior for (1) Ceres deduced from its gravity field and shape. Nature. 2016; doi: 10.1038/nature18955

Peplowski PN, Klima RL, Lawrence DJ, Ernst CM, Denevi BW, Frank EA, Goldsten JO, Murchie SL, Nittler LR, Solomon SC. Remote sensing evidence for an ancient carbon-bearing crust on Mercury. Nature Geoscience. 2016; 9(4):273–+. DOI: 10.1038/NGEO2669

Pieters, CM., Garrick-Bethell, I. Hydration Variations at Lunar Swirls. 46th Lunar and Planetary Science Conference; Abstract #2120, Lunar and Planetary Institute, Houston. 2015.

Pieters CM, Taylor LA, Noble SK, Keller LP, Hapke B, Morris RV, Allen CC, McKay DS, Wentworth S. Space weathering on airless bodies: Resolving a mystery with lunar samples. Meteorit Planet Sci. 2000; 35(5):1101–1107. doi:10.1111/j.1945- 5100.2000.tb01496.x.

Pieters C, Goswami J, Clark R, Annadurai M, Boardman J, Buratti B, Combe JP, Dyar M, Green R, Head J. Character and spatial distribution of OH/H2O on the surface of the Moon seen by M3 on Chandrayaan-1. Science. 2009; 326(5952):568–572. DOI: 10.1126/science.1178658 [PubMed: 19779151]

Pieters CM, et al. Distinctive space weathering on Vesta from regolith mixing processes. Nature. 2012; 491(7422):79–82. DOI: 10.1038/Nature11534 [PubMed: 23128227]

Pieters, CM., Moriarty, DPI., Garrick-Bethell, I. Atypical Regolith Processes Hold the Key to Enigmatic Lunar Swirls. 45th Lunar and Planetary Science Conference; Abstract #1408, Lunar and Planetary Institute, Houston. 2014a.

Pieters CM, Murchie S, Thomas N, Britt D. Composition of Surface Materials on the Moons of Mars. Planet Space Sci. 2014b; 102:144–151. DOI: 10.1016/J.Pss.2014.02.008

Pieters, CM., et al. Surface Processes and Space Weathering on Ceres. 47th Lunar and Planetary Science Conference; Abstract #1383, Lunar and Planetary Institute, Houston. 2016.

Prettyman TH, et al. Elemental Mapping by Dawn Reveals Exogenic H in Vesta's Regolith. Science. 2012; 338(6104):242–246. DOI: 10.1126/science.1225354 [PubMed: 22997135]

Ramsley KR, Head JW. Mars impact ejecta in the regolith of Phobos: Bulk concentration and distribution. Planet Space Sci. 2013; 87:115–129. DOI: 10.1016/J.Pss.2013.09.005

Roberts JH, Kahn EG, Barnouin OS, Ernst CM, Prockter LM, Gaskell RW. Origin and flatness of ponds on asteroid 433 Eros. Meteorit Planet Sci. 2014; 49(10):1735–1748. DOI: 10.1111/maps.12348

Robinson MS, Thomas PC, Veverka J, Murchie S, Carcich B. The nature of ponded deposits on Eros. Nature. 2001; 413(6854):396–400. DOI: 10.1038/35096518 [PubMed: 11574881]

Robinson MS, et al. Reflectance and color variations on Mercury: Regolith processes and compositional heterogeneity. Science. 2008; 321(5885):66–69. DOI: 10.1126/Science.1160080 [PubMed: 18599770]

Rosenblatt P. The origin of the martian moons revisited. Astron Astrophys Rev. 2011; 19(1):19–44.

Rout SS, Moroz LV, Baither D, van der Bogert CH, Bischoff A. Laboratory simulations of space weathering and impact heating of planetary surfaces: the TEM studies. European Planetary Science Congress. 2008; 1:941. Abstracts.

Russell CT, et al. Dawn completes its mission at 4 Vesta. Meteorit Planet Sci. 2013; 48(11):2076–2089. DOI: 10.1111/Maps.12091

Russell CT. Dawn Arrives at Ceres: Exploration of a Small Volatile-Rich World. Science. 2016 in press.

Sasaki S, Nakamura K, Hamabe Y, Kurahashi E, Hiroi T. Production of iron nanoparticles by laser irradiation in a simulation of lunar-like space weathering. Nature. 2001; 410:555–557. DOI: 10.1038/35069013 [PubMed: 11279486]

Sasaki S, Kurahashi E, Yamanaka C, Nakamura K. Laboratory simulation of space weathering: Changes of optical properties and TEM/ESR confirmation of nanophase metallic iron. Advances in Space Research. 2003; 31(12):2537–2542. DOI: 10.1016/S0273-1177(03)00575-1

Simone M, Stefano M, Gabriele C, Matteo M, Elena M. A New Chronology for the Moon and Mercury. The Astronomical Journal. 2009; 137(6):4936.doi: 10.1088/0004-6256/137/6/4936

Sunshine JM, Farnham TL, Feaga LM, Groussin O, Merlin F, Milliken RE, A'Hearn MF. Temporal and spatial variability of lunar hydration as observed by the Deep Impact spacecraft. Science. 2009; 326(5952):565–568. DOI: 10.1126/science.1179788 [PubMed: 19779149]

Syal MB, Schultz PH. Cometary impact effects at the Moon: Implications for lunar swirl formation. Icarus. 2015; 257:194–206. DOI: 10.1016/j.icarus.2015.05.005

Syal MB, Schultz PH, Riner MA. Darkening of Mercury's surface by cometary carbon. Nature Geoscience. 2015; 8(5):352–356. DOI: 10.1038/ngeo2397

Taylor LA, Pieters CM, Keller LP, Morris RV, McKay DS. Lunar Mare Soils: Space weathering and the major effects of surface-correlated nanophase Fe. J Geophys Res-Planet. 2001; 106(E11): 27985–27999. DOI: 10.1029/2000je001402

Taylor LA, Pieters C, Patchen A, Taylor DHS, Morris RV, Keller LP, McKay DS. Mineralogical and chemical characterization of lunar highland soils: Insights into the space weathering of soils on airless bodies. Journal of Geophysical Research: Planets. 2010; 115(E2):E02002.doi: 10.1029/2009JE003427

Thomas N, Stelter R, Ivanov A, Bridges NT, Herkenhoff KE, McEwen AS. Spectral heterogeneity on Phobos and Deimos: HiRISE observations and comparisons to Mars Pathfinder results. Planetary and Space Science. 2011; 59:1281–1292. DOI: 10.1016/j.pss.2010.04.018

Tompkins S, Pieters CM. Spectral characteristics of lunar impact melt and inferred mineralogy. Meteoritics and Planetary Science. 2010; 45(7):1152–1169. DOI: 10.1111/j.1945-5100.2010.01074.x

Trombka JI, et al. The Elemental Composition of Asteroid 433 Eros: Results of the Near-Shoemaker X-ray Spectrometer. Science. 2000; 289:2101–2105. [PubMed: 11000107]

Tsuchiyama A, et al. Three-Dimensional Structure of Hayabusa Samples: Origin and Evolution of Itokawa Regolith. Science. 2011; 333(6046):1125–1128. DOI: 10.1126/science.1207807 [PubMed: 21868671]

Tsuchiyama A. Asteroid Itokawa A Source of Ordinary Chondrites and A Laboratory for Surface Processes. Elements. 2014; 10(1):45–50. DOI: 10.2113/gselements.10.1.45

Vander Kaaden KE, McCubbin FM. Exotic crust formation on Mercury: Consequences of a shallow, FeO-poor mantle. J Geophys Res-Planet. 2015; 120(2):195–209. DOI: 10.1002/2014JE004733

Wehner GK. Sputtering Effects on the Moon's Surface. Am Rocket Soc Journal. 1961; 31(3):438–439. DOI: 10.2514/8.5498

Wehner, GK. Sputtering Effects On The Lunar Surface. In: Salisbury, J., Glaser, PE., editors. The Lunar Surface Layer. Academic Press; 1964. p. 313-322.

Weider SZ, Nittler LR, Starr RD, McCoy TJ, Solomon SC. Variations in the abundance of iron on Mercury's surface from MESSENGER X-Ray Spectrometer observations. Icarus. 2014; 235:170–186. DOI: 10.1016/j.icarus.2014.03.002

Wieser M, Barabash S, Futaana Y, Holmström M, Bhardwaj A, Sridharan R, Dhanya MB, Schaufelberger A, Wurz P, Asamura K. First observation of a mini-magnetosphere above a lunar

magnetic anomaly using energetic neutral atoms. Geophysical Research Letters. 2010; 37(5):n/a–n/a. DOI: 10.1029/2009GL041721

Yamada M, Sasaki S, Nagahara H, Fujiwara A, Hasegawa S, Yano H, Hiroi T, Ohashi H, Otake H. Simulation of space weathering of planet-forming materials: Nanosecond pulse laser irradiation and proton implantation on olivine and pyroxene samples. Earth, Planets and Space. 1999; 51(11):1255–1265. DOI: 10.1186/bf03351599

Yano H, et al. Touchdown of the Hayabusa Spacecraft at the Muses Sea on Itokawa. Science. 2006; 312(5778):1350–1353. DOI: 10.1126/science.1126164 [PubMed: 16741113]

Zakharov A, Horanyi M, Lee P, Witasse O, Cipriani F. Dust at the Martian moons and in the circummartian space. Planet Space Sci. 2014; 102:171–175. DOI: 10.1016/j.pss.2013.12.011

Zhang, S., Keller, LP. Space Weathering Effects in Lunar Soils: The Roles of Surface Exposure Time and Bulk Chemical Composition. 42nd Lunar and Planetary Science Conference; Abstract #1947, Lunar and Planetary Institute, Houston. 2011.

Zinner, E. On the constancy of solar particle fluxes from track, thermoluminescence and solar wind measurement in lunar rocks. In: Pepin, RO.Eddy, JA., Merrill, RB., editors. The Ancient Sun: Fossil Record in the Earth, Moon and Meteorites. Pergamon, New York: 1980. p. 201-226.

Three Key Points

- Bodies exposed to the space environment are altered with time.
- The type and magnitude of alteration depends on composition and location.
- Understanding the physics and chemistry of space weathering processes are areas of active research.

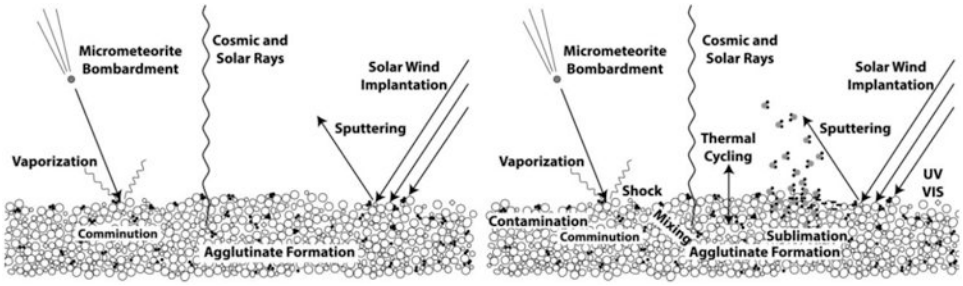

Figure 1.

The complex array of processes involved in space weathering of airless bodies. Typical soils are particulate but heterogeneous in composition. (Left) Dominant processes affecting the surface of the Moon at 1 AU [after Noble 2004]. (Right) The broad range of surfaces processes now believed to be active across the solar system, but with different degrees of prominence for specific environments.

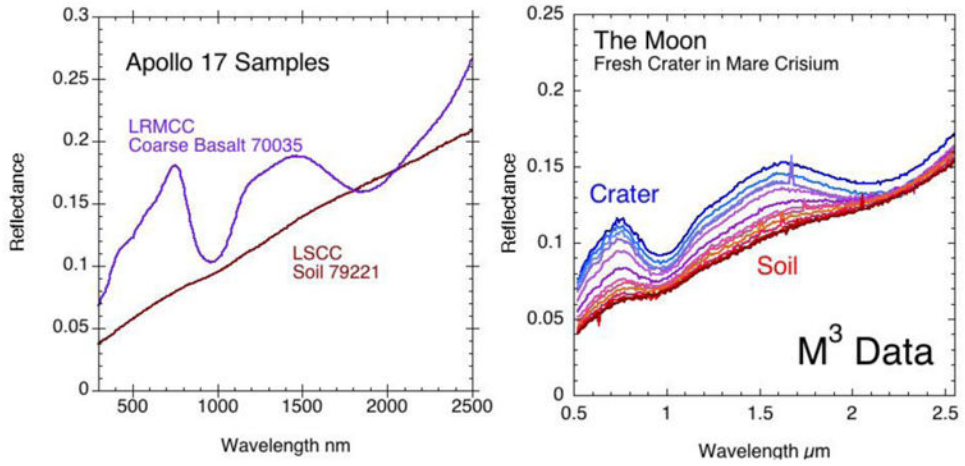

Figure 2.

Spectra of lunar materials illustrating the optical differences between fresh rocks and well developed lunar soils. Left) Laboratory spectra of basaltic lunar rock and soil samples from Apollo 17 (RELAB data: LR-CMP-158 and LR-CMP-039). Right) Remote lunar spectra acquired from orbit with Moon Mineralogy Mapper (M^3) as a traverse from a mare basalt small fresh crater into surrounding well-developed soil (M^3 file M3T20090701T094734). For these basalt examples, diagnostic absorption bands are stronger for fresh materials, but note the prominent differences in brightness at visible wavelengths (500-700nm), but little if any brightness difference near 2 μm.

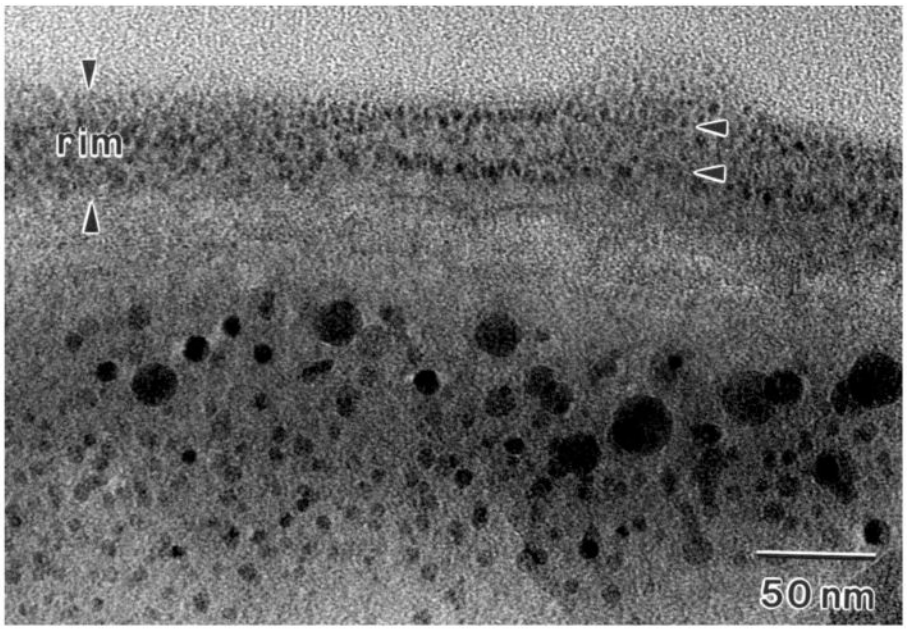

a.

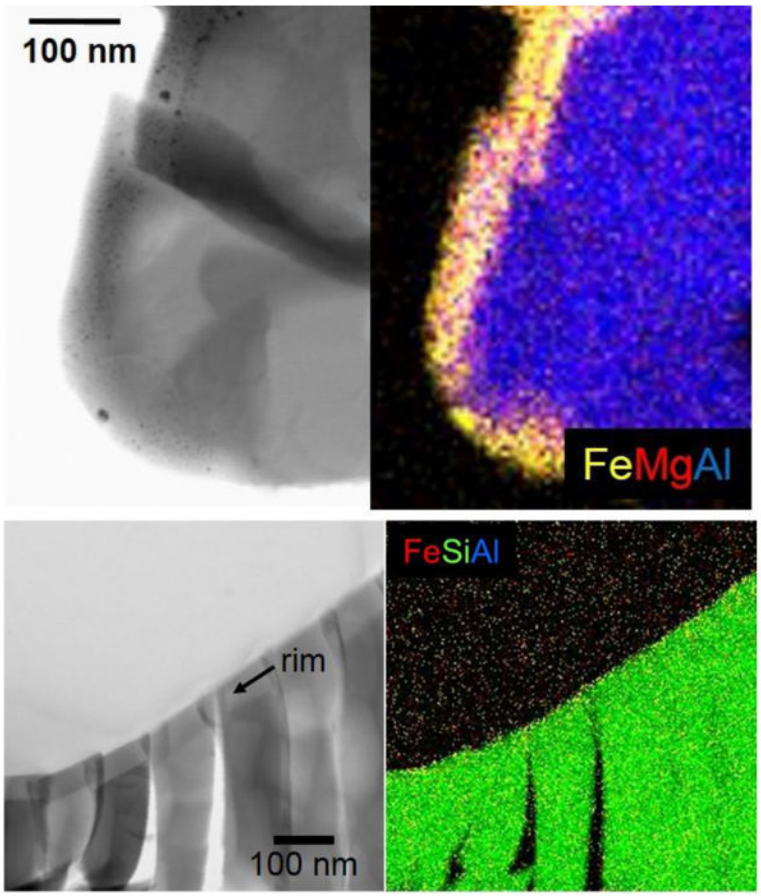

b.

Figure 3.

a. TEM image of a lunar agglutinate illustrating the presence of npFe^0 forming two layers within the rim, but larger Fe^0 in the interior. b. TEM bright field images and chemical maps of typical lunar soil rims. The plagioclase grain (top) has a depositional npFe-rich rim, which is chemically distinct from the host grain. The cristobalite grain (bottom) has an amorphous solar-wind damage rim compositionally indistinguishable from the host grain. (Images courtesy: Lindsay Keller)

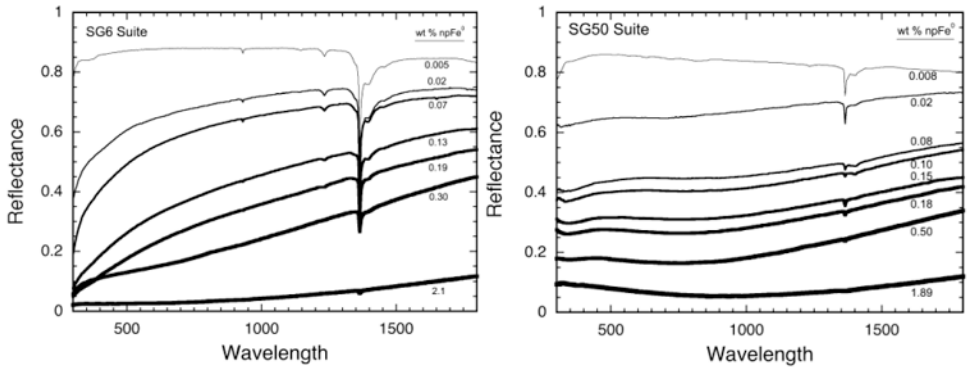

Figure 4.

Silica gels impregnated with varying amounts of optically active iron particles. The SG6 suite, which contains metallic iron with a range of ~10-25 nm diameter, shows significant reddening, while the SG50 suite, with a range of 20-200 nm particles, shows significant darkening, but little reddening. (These and related spectra from [Noble *et al.,* 2007] can be found in the RELAB data files as samples SN-CMP-014 to SN-CMP-145.)

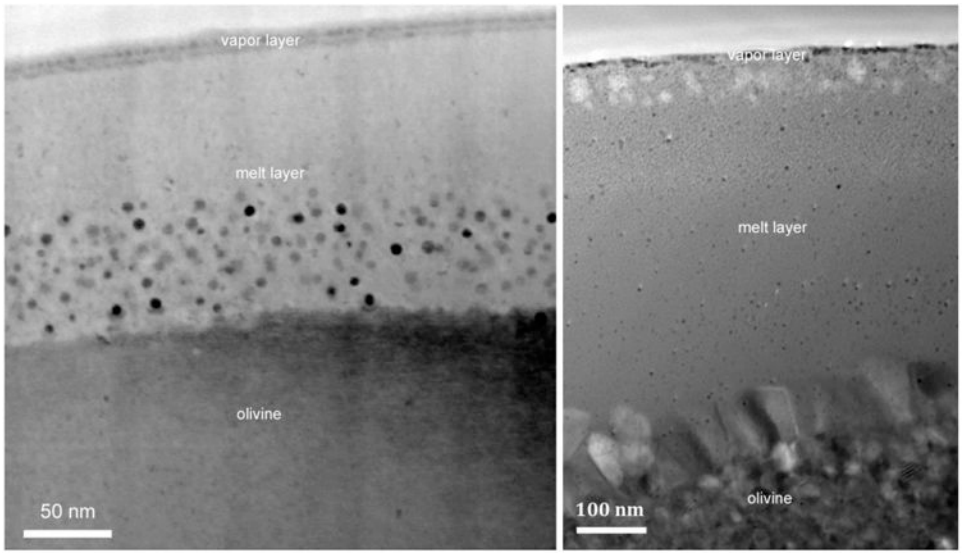

Figure 5.

TEM analysis demonstrates that nanophase iron is produced in the melt and vapor of both experimentally laser irradiated (left) [Noble *et al.,* 2011] and natural micrometeoroid impacts into olivine (right) [Noble *et al.,* 2016].

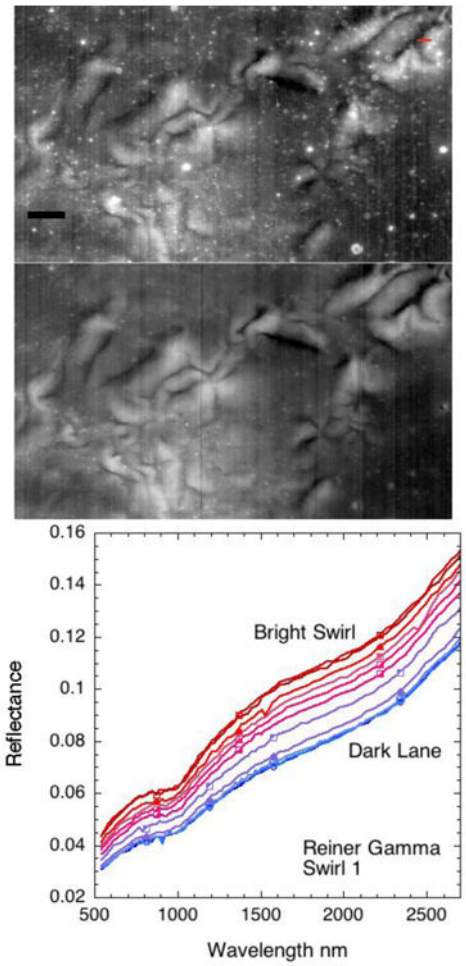

Figure 6.

M^3 images and spectra across a lunar swirl region south west of central Reiner Gamma. [Left] M^3 reflectance images obtained at 750 nm (top) illustrating albedo variations at visible wavelengths, and at 2200 nm (bottom) illustrating that the swirl albedo features persist into the near-infrared, but the fresh crater features do not. [Right] M^3 traverse of spectra across a dark lane into the bright swirl (location shown with small red line in upper right corner of 750 nm image). The example traverse across this Reiner Gamma swirl in a mare region illustrates that the bright swirl areas exhibit properties that are quite different from immature (unweathered) soils such as found at typical mare craters (see for comparison Figure 2 above). Scale bar is 5 km. (M^3 images and spectra are from M3G20090613T032520 and M3G20090613T073612.)

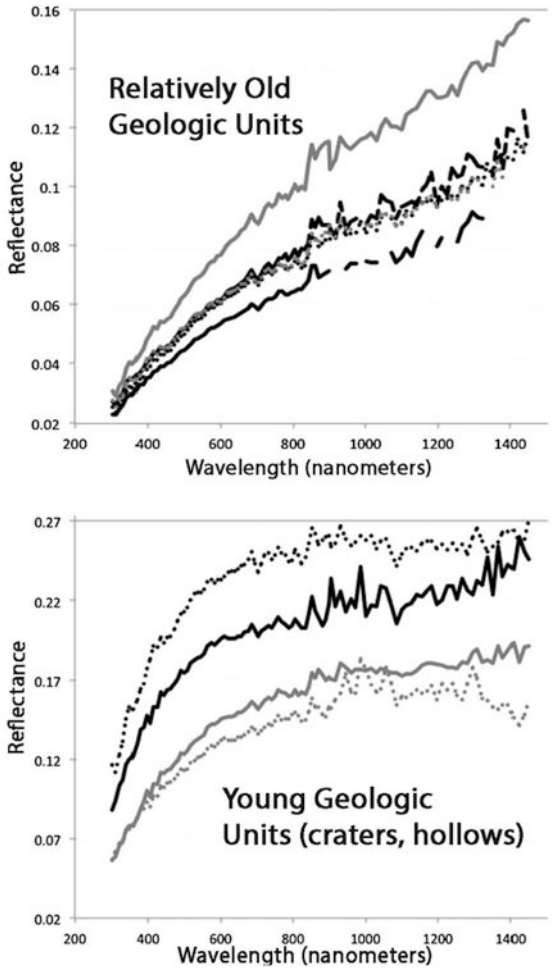

Figure 7.

Comparison of spectra for units of Mercury obtained by Mercury Atmospheric and Surface Composition Spectrometer (MASCS) on MESSENGER [Domingue *et al.*, 2014 and Izenberg *et al.*, 2014]. The vertical scale for the young units is almost 2× that of the older units. Although major mineral/amorphous components of the surface are poorly understood, the optical relation between young and older units directly mimics that seen experimentally with a combination of nanophase and Britt-Pieters opaque particles [e.g., Noble *et al.,* 2007].

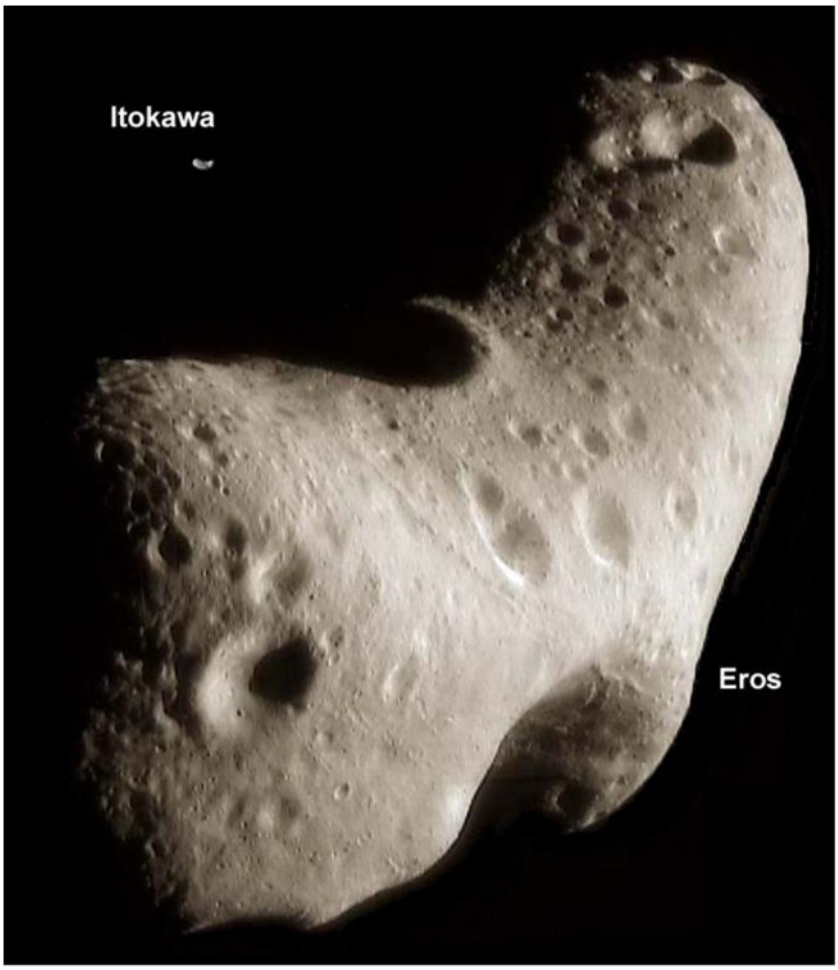

Figure 8.
Eros and Itokawa to scale

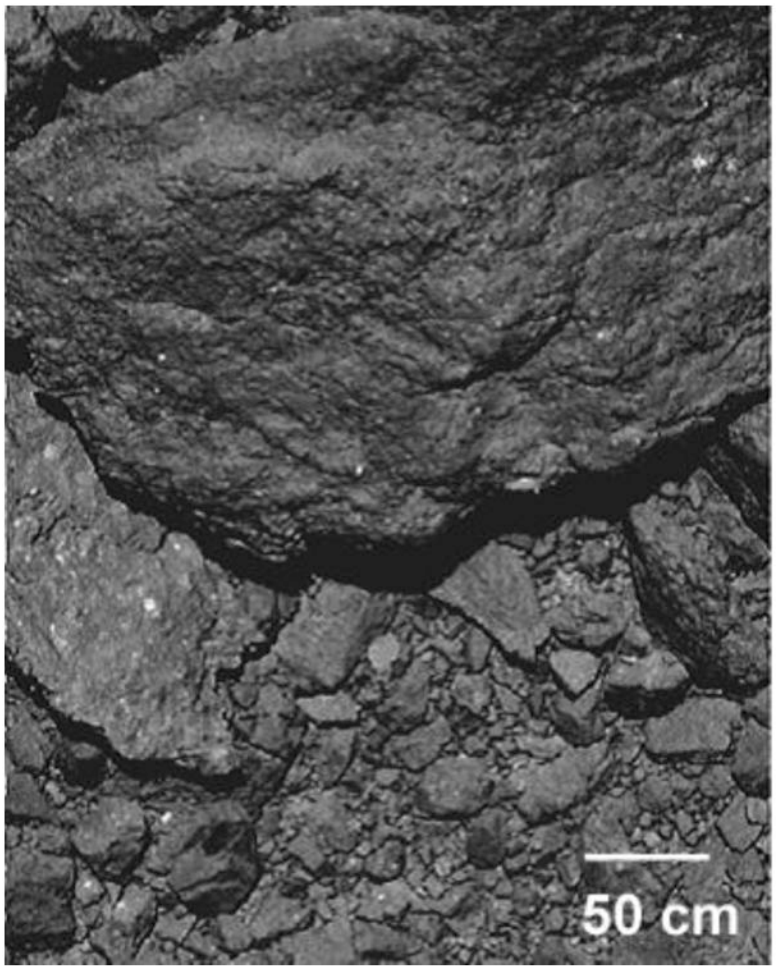

Figure 9.
Bright spots can be seen in this close up of the rocky surface of Itokawa obtained by Hayabusa (ST_2544579522), these presumably represent recent impacts that have penetrated through the darkened patina surface to the brighter fresh rock below.

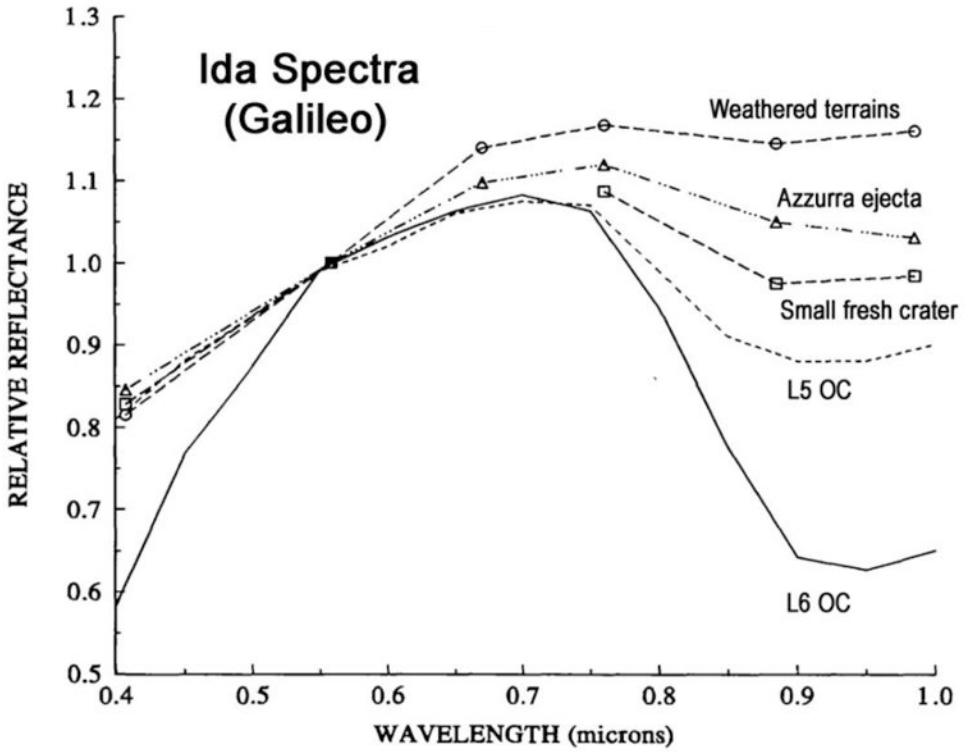

Figure 10.

Weathering trends on Ida exhibited with 6-band reflectance spectra obtained by the Galileo mission compared with ordinary chondrite (OC) spectra. Fresh (younger) features have deeper ferrous absorption bands. The weathered terrains have a steeper continuum (red sloped) and have weaker bands. After Chapman [1996].

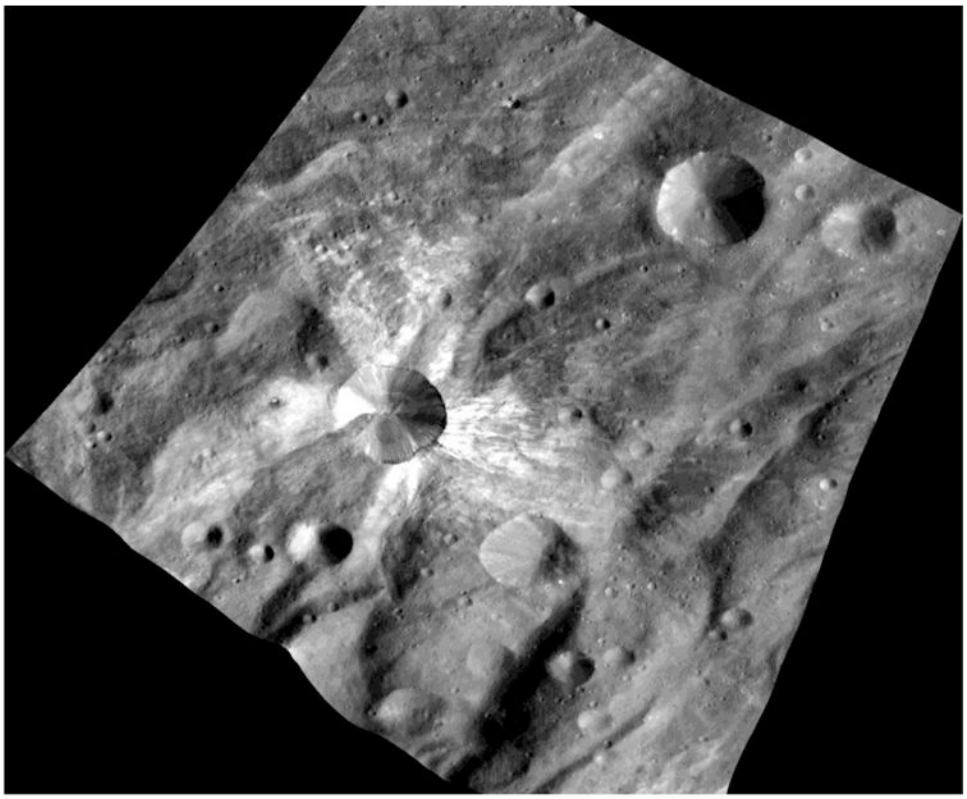

Figure 11.
Image of the surface of Vesta obtained by Dawn Framing Camera (FC21B0010859_11293124257F1A) containing two ~10 km craters. The crater to the southwest exhibits classic features of a fresh impact crater (sharp rim, diverse surrounding ray system). The older impact crater to the northeast exhibits more subdued features and rays have been removed by local space weathering believed to be dominated by regolith mixing and gardening.

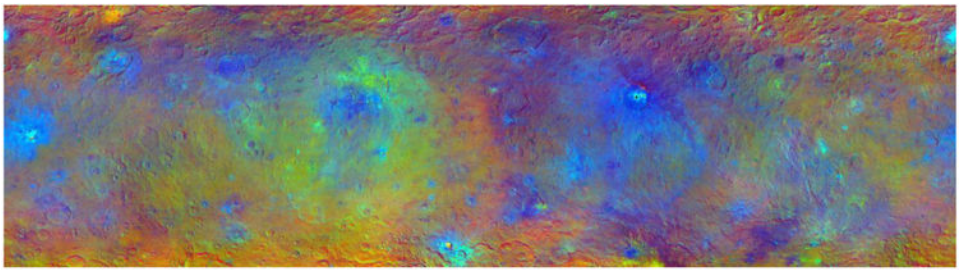

Figure 12.

Color composite image of Ceres 60°N to 50°S latitude, 0° to 360° longitude compiled from Dawn Framing Camera data using R=965/750 nm, G=750 nm; B=440/750 nm. This representation enhances subtle color and albedo variations across the surface (a ‘blue’ spectral slope across the visible thus appears blue). Most fresh craters appear relatively blue and some exhibit extensive ray patterns.

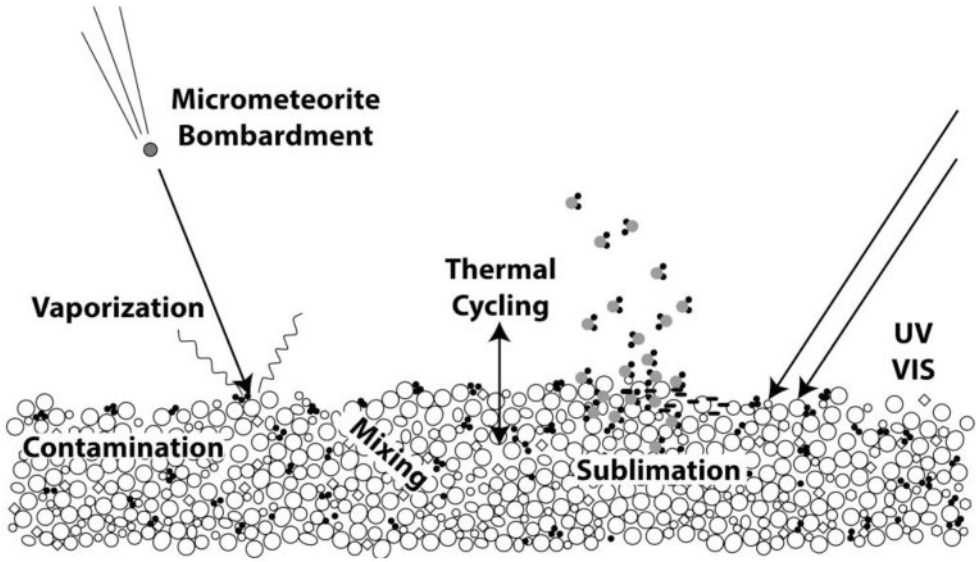

Figure 13.

Processes involved in space weathering of Ceres. Because the environment is so unlike that at 1 AU, the dominant processes are distinctly different and include contamination and mixing with exogenic material as well as formation of a surficial lag deposit as volatile materials sublimate or are lost.

Figure 14.

Enhanced false color image of the Mars-side of Phobos obtained by HiRISE [PSP_007769_9010_IRB] illustrating the relation between two different units that are either compositionally distinct or represent different degrees of space weathering alteration. Although spatially coherent, most of the color difference observed reflect variations in overall continuum slope with the most extensive material being a steeply sloped ‘red’ unit [e.g., Pieters *et al.,* 2014]. Processing of this image is described in Thomas *et al.* [2010] from three broad band filters with effective wavelengths being ~ R=874 nm, G=694, B=536 nm.